

<https://helda.helsinki.fi>

Microbial Community Composition Correlates with Metal Sorption in an Ombrotrophic Boreal Bog : Implications for Radionuclide Retention

Lusa, Merja

Multidisciplinary Digital Publishing Institute

2021-03-19

Lusa, M.; Bomberg, M. Microbial Community Composition Correlates with Metal Sorption in an Ombrotrophic Boreal Bog: Implications for Radionuclide Retention. *Soil Syst.* 2021, 5, 19.

<http://hdl.handle.net/10138/328390>

Downloaded from Helda, University of Helsinki institutional repository.

This is an electronic reprint of the original article.

This reprint may differ from the original in pagination and typographic detail.

Please cite the original version.

Article

Microbial Community Composition Correlates with Metal Sorption in an Ombrotrophic Boreal Bog: Implications for Radionuclide Retention

Merja Lusa ^{1,*} and Malin Bomberg ² 
¹ Department of Chemistry, Radiochemistry, Faculty of Science, University of Helsinki, 00014 Helsinki, Finland

² VTT Technical Research Centre of Finland, Tietotie 2, 02150 Espoo, Finland; malin.bomberg@vtt.fi

* Correspondence: merja.lusa@helsinki.fi

Abstract: Microbial communities throughout the 6.5 m depth profile of a boreal ombrotrophic bog were characterized using amplicon sequencing of archaeal, fungal, and bacterial marker genes. Microbial populations and their relationship to oxic and anoxic batch sorption of radionuclides (using radioactive tracers of I, Se, Cs, Ni, and Ag) and the prevailing metal concentrations in the natural bog was investigated. The majority of the detected archaea belonged to the Crenarchaeota, Halobacterota, and Thermoplasmatota, whereas the fungal communities consisted of Ascomycota, Basidiomycota, and unclassified fungi. The bacterial communities consisted mostly of Acidobacteriota, Proteobacteria, and Chloroflexi. The occurrence of several microbial genera were found to statistically significantly correlate with metal concentrations as well as with Se, Cs, I, and Ag batch sorption data. We suggest that the metal concentrations of peat, gyttja, and clay layers affect the composition of the microbial populations in these nutrient-low conditions and that particularly parts of the bacterial and archaeal communities tolerate high concentrations of potentially toxic metals and may concurrently contribute to the total retention of metals and radionuclides in this ombrotrophic environment. In addition, the varying metal concentrations together with chemical, mineralogical, and physical factors may contribute to the shape of the total archaeal and bacterial populations and most probably shifts the populations for more metal resistant genera.

Keywords: microbial communities; heavy metal tolerance; boreal environment; radionuclide sorption



Citation: Lusa, M.; Bomberg, M. Microbial Community Composition Correlates with Metal Sorption in an Ombrotrophic Boreal Bog: Implications for Radionuclide Retention. *Soil Syst.* **2021**, *5*, 19. <https://doi.org/10.3390/soilsystems5010019>

Academic Editor: Heike Knicker

Received: 3 February 2021

Accepted: 16 March 2021

Published: 19 March 2021

Publisher's Note: MDPI stays neutral with regard to jurisdictional claims in published maps and institutional affiliations.



Copyright: © 2021 by the authors. Licensee MDPI, Basel, Switzerland. This article is an open access article distributed under the terms and conditions of the Creative Commons Attribution (CC BY) license (<https://creativecommons.org/licenses/by/4.0/>).

1. Introduction

Heavy metals and radionuclides polluting the environment originate mainly from anthropogenic sources, including uranium mining, coal combustion, and accidental or purposeful release of radionuclides. Heavy metals and radioactive isotopes may present variable threats to biota, due to, e.g., atmospheric deposition and enrichment in soils and sediments, build-up into water bodies, and their high toxicity [1–6]. Radioactive isotopes and heavy metals can have toxic effects on soil microorganism activity if bioavailable and present in sufficient concentrations [7]. Heavy metals may also inhibit the growth and vitality of microorganisms and cause changes in the community structure [6,8].

In the Finnish concept for the disposal of spent nuclear fuel, the fuel will be placed in copper-sheeted canisters and disposed of in a deep bedrock repository constructed on Olkiluoto Island. During the last glacial period, this area was covered by the Scandinavian Ice Sheet and after the ice retreated, gradual post-glacial land uplift still continues in the area. The land uplift will result in a formation of new bogs in the area on which the first possible releases from the deep nuclear repository to the upper biosphere (through the clay, gyttja and peat layers in this order) would, based on biosphere safety assessment calculations, be possible if some of the copper canisters would leak. The Lastensuo Bog, sampled in our study, approximates the bog type likely to form in this area and has therefore been used as an analogue biotope in the biosphere safety assessments of the

disposal of spent nuclear fuel in Finland [9]. ^{59}Ni , $^{108\text{m}}\text{Ag}$, ^{135}Cs , ^{79}Se , and ^{129}I , with calculated potential geosphere release rates between 10^1 and 10^3 Bq/a starting 10^3 years after the start of disposal, are among the most important radionuclides, as the potential radiation doses for humans in the biosphere safety assessment calculations of spent nuclear fuel are considered [10].

Non-radioactive Ni may end up in the environment from antropogenic sources, see, e.g., in [11–14]. Ni occurs in several forms in soils, e.g., as inorganic crystalline minerals or precipitates, adsorbed or complexed on various organic or inorganic cation exchange surfaces, chelated to metal complexes in soil solution where a decrease in soil pH increases its mobility, or as a water-soluble free ion [15]. From the radioecological point of view, radioactive isotope of Ni, ^{59}Ni , with long half-life of 76,000 years has classified as one of the high priority radionuclides in the biosphere safety assessments of the disposal of SNF in Finland due to the high calculated potential biosphere release rates of this nuclide (maximum of $\sim 10^3$ Bq a^{-1} at $t = 10^5$ years after the beginning of the disposal) [10]. Ni has high metabolic impact on living organisms because it is an important component in many enzymes [16,17]. In addition, many microorganisms can bind Ni by using various uptake mechanisms, including intracellular accumulation, straight biosorption on cell surfaces (through physical adsorption, complexation, or ion-exchange), and extracellular precipitation [18–22]. Retardation may occur through cell surface metal-binding functional groups, like carboxyl, hydroxyl, phosphate, and sulfate groups [18–20]. In addition, many microbes are able to accumulate Ni also inside the cells (see, e.g., in [22]) and until this date at least two different uptake mechanisms have been reported: ATP-binding cassette (ABC-type) transporters as well as Ni-specific permeases [23]. The possible toxic effects of Ni may be suppressed during active accumulation inside bacterial cells through detoxification reactions and previously we observed that Ni(II) concentrations between 0.01 and 1 mM had no toxic effects on *Pseudomonas* sp. strains isolated from the same Lastensuo Bog [22] studied in present study.

Silver (Ag) has been released to the biosphere especially through the photographic and imaging industry [24]. Ag is a non-essential metal with a high toxicity to many organisms already at very low concentrations [25] and is used as an effective bactericide [26,27]. Ag accumulates effectively in food chains and can cause various diseases and disorders, and even death [28–30]. It has been estimated that 5% of the total soil Ag is bioavailable [25]. In heavily contaminated soils, this proportion may be enough to harmfully affect the soil micro- and macrobiological populations. The radioisotope of Ag, $^{108\text{m}}\text{Ag}$ ($T_{1/2}$ 418 years), is found in SNF and is assumed to be one of the instant release fraction (IRF) radionuclides if the copper canisters of the SNF are compromised and thus $^{108\text{m}}\text{Ag}$ can cause a substantial part of the radiation dose from potentially released SNF to the biosphere [31].

Radioisotopes of cesium, including ^{137}Cs and ^{135}Cs , are typically considered a greater health risk than stable cesium [32]. In soils, cesium is relatively rare and the stable cesium (^{133}Cs) concentrations are roughly 5 mg/kg [33]. In addition to the above-mentioned isotopes of Ni and Ag, ^{135}Cs , with its long half-life of 2.3 My and large inventory in SNF, is also among the most important radionuclides in the SNF repository long-term biosphere safety assessments [34]. Typical for alkali metals, cesium is highly soluble and therefore in SNF it is expected to occur in the instant release fraction [33]. Cesium occurs at oxidation state I (Cs^+), and in soils it is typically sorbed by outer-sphere complexation, although in mica and clay minerals also inner-sphere complexes are formed [34–36]. In addition, cesium retains, e.g., on organic matter and on iron, manganese and aluminum oxides. Bacteria, including boreal *Pseudomonas* sp., *Paenibacillus* sp., *Burkholderia* sp., *Rhodococcus* sp. [37] and anaerobic iron- and sulfate-reducing bacterial mixtures [38] have been reported to accumulate low (K_d values below 100 L/kg) concentrations of cesium. Arbusculat mycorrhizal fungi have been shown to facilitate the uptake of the radioactive ^{137}Cs and translocate it to a plant host [39] or concentrate in the fungal fruiting bodies [40]. Mycorrhizal fungi have also been shown to transport radio-cesium between plant individuals connected via the same hyphal network [41].

^{79}Se is a high-priority radionuclide in the long-term safety assessments of the disposal of SNF into deep bedrock repositories [33]. Therefore, the possible radiation doses caused by radioactive selenium for humans are taken into consideration in the long-term safety calculations of SNF disposal [33]. The radioactive selenium isotope ^{79}Se ($T_{1/2}$ 65,000 years) is a fission product of uranium used in nuclear reactors and is also formed by neutron activation from stable selenium. Moreover, substantial amounts of stable selenium enter the biosphere through anthropogenic activities including coal combustion, mining, refining of sour crude oils, and agricultural irrigation of seleniferous soils [42–46]. Selenium is a vital micronutrient for humans and other mammals, but it is toxic at higher concentrations and the range between deficient and toxic doses is characteristically narrow [47,48]. For humans, the effective daily dietary doses vary between 40 and 400 μg per day [49] and the mean abundance of selenium in the soil crust is 0.083 mg/kg [50]. In most soils, its concentrations are between 0.1 and 2 mg/kg [51]. However, exceptionally high Se concentrations up to 1200 mg/kg have been reported from different areas of the world (like organic-rich soils in Ireland) [52]. In soils, selenium occurs in different oxidation states, and in alkaline agricultural soils, selenium mainly occurs as selenate (Se(VI) , SeO_4^{2-}) as for acidic forest soils its most profound form is selenite (Se(IV) , SeO_3^{2-}) [52]. The retention and mobility of selenium is dependent, in addition to other factors like pH and organic matter content of the soil, on its speciation [53]. Especially, selenite is highly reactive and may react with glutathione thiol groups (GSH), explaining, at least in partly, its toxicity [54]. Selenite spontaneously reacts with glutathione producing, e.g., glutathioselenol and selenodiglutathione [55]. It has been also reported that different species of Se-reducing bacteria produce elemental Se^0 biominerals, which can have different atomic structures [56,57]. In soils, selenite and selenate are quickly reduced (also under oxic conditions), and this occurs mostly through microbial reduction [58–60]. Certain bacteria may use selenate and selenite as terminal electron acceptor [61] and may facilitate selenium uptake in plants [62,63]. Fungi have also been found to reduce selenite and selenate in oxic conditions [64]. In addition, under highly reducing conditions slow abiotic reduction is mediated by inorganic Fe(II,III) [65]. Previously, we showed that *Pseudomonas* sp. strains isolated from the same Lastensuo bog as was studied in the present study, were able to reduce selenite at 6 mM concentrations into reduced elemental selenium inside the bacterial cells even though the bacterial growth rate (as increased lag phase duration) was affected by the Se(IV) amendment [63].

^{129}I , with its very long half-life of 15.7 My, large inventory in SNF, and high mobility, is one of the most significant radionuclides in the long-term safety assessments of SNF [33]. Iodine is also vastly biophilic, and via the food chain or by inhalation can bioaccumulate, particularly in the thyroid glands of both humans and other mammals [48]. The migration and sorption behavior of iodine in the bio- and geosphere is affected by several factors, such as chemical speciation, organic matter content, mineral properties, redox potential, pH, and microorganisms [66–71]. Although iodine is primarily retained in soil organic matter (SOM) [72–76], microorganisms may affect its sorption, see, e.g., in [77–79].

Copper may also leach into the biosphere from the spent nuclear fuel canisters (the copper canisters in the KBS-3 model) through both abiotic and microbially induced corrosion mechanisms [80,81], locally increasing the environmental Cu load. Cu is a cofactor in many enzymes and is an essential micronutrient but is generally toxic to microorganisms, see, e.g., in [82,83]. However, many microorganisms have developed resistance mechanisms for coping with elevated Cu concentrations [83,84]. Elevated concentration is a relative term, but for, e.g., *E. coli*, the minimal inhibitory concentration (MIC) of Cu^{2+} has been determined to be 1 mM [85].

The resident microbial community has different mechanisms to interact with radionuclides and heavy metals, including biosorption, accumulation, precipitation, enzymatic transformations (redox reactions), and detoxification reactions [84–86]. Biosorption may occur both in living cells as well as in dead cells and cell fragments, but other mechanisms in which uptake occurs through active biological processes are present only in

living cells [84,86,87]. For example, in prokaryotic cells, Ni and Se can be transported inside the cells using ABC transporters [84,87]. In the active uptake mechanisms, Ni is incorporated into Ni-dependent enzymes like urease, carbon monoxide dehydrogenase or certain superoxide dismutases and methylenediureases [84]. In the case of Se, the use of various enzymes like sulfite reductases and OYE enzymes is also possible [87], and often uptake is followed by detoxification reactions utilizing reduction (see, e.g., in [58,64]). For iodine, bacterial oxidation processes are well documented (see, e.g., in [88–91]) and H₂O₂-dependent iodide oxidation mechanism has been reported, e.g., in bacteria from the Savannah River Site [72]. In soil, organic matter iodine sorption has been suggested to occur through catalytic oxidation of I[−] into reactive iodine species, such as I₂ and HIO, by environmental (microbial) peroxides, which after reactive iodine is bound into organic matter [80]. However, uptake (probably through I₂ and HIO oxidation) of iodine has been described in fewer studies (see, e.g., in [88,92–94]). However, filamentous fungi have also been shown to bioaccumulate both iodide and iodate, but the mobilization of iodate is more efficient [95]. Typical for the metabolism-dependent mechanisms is that they are slower than biosorption on cell walls [22]. Bacterial and fungal surfaces contain multiple functional groups that may serve as sites for adsorption (and possibly subsequent desorption) (see, e.g., in [96,97]). Such functional groups, found both in Gram-negative and in Gram-positive bacteria, may be carboxylic, phosphate, and hydroxyl sites that deprotonate with increasing pH and therefore straight sorption on to the cellular structures is considered pH dependent [98]. On these sites the uptake follows the displacement of protons and therefore depends on the protonation [99,100]. However, typical bacterial cells have high buffering capacity, which can range, e.g., through the whole environmentally relevant pH range from pH 3 to pH 9 [100]. Vast prokaryotic buffering capacity results from distinct acidic sites that are located in the cell walls [100] and is of great importance in changing environmental conditions. Microorganisms also have mechanisms for removing heavy metals, metalloids and transition metals from their cells, by using e.g., ATP-coupled pumps more or less specific for different ions, such as copper or silver ATPase transporters in bacteria, archaea and fungi [101–103].

In the present study, the objective was to study the effects of the total microbiome on the sorption behavior of the radioactive isotopes of Ni, Ag, Se, I, and Cs in an ombrotrophic boreal bog, and vice versa. In addition, the relationship between the microbiome and measured soil metal concentrations and correlations between soil metal concentrations, pH, water content and organic matter content and bacterial, archaeal, and fungal populations was studied.

2. Materials and Methods

2.1. Sampling Site and Sample Pretreatment

The sampling site, Lastensuo Bog, is an ombrotrophic, nutrient-poor bog with a maximum peat thickness of 5–6 m with a bottom soil consisting of gyttja and clay [9,104]. The bog is located on the western coast of Finland and our sampling point (Figure 1, WGS84 coordinates 61°17′31″ N, 21°50′22″ E) is located in the center parts of the bog, which consist of treeless or near treeless *Sphagnum fuscum* bog. The surrounding bog area also contain ridge hollow pine bog and hollow bog, with low sedge bog, cotton grass pine bog, tall sedge pine fen, and forested peatland at the edges [105]. The main peat types include *Sphagnum* peat (58%), sedge peat (19%), and few-flowered sedge (15%).

Discontinuous depth-wise samples of peat, gyttja and clay for oxic and anoxic studies were obtained in 2013 [80]. In addition, surface *Sphagnum* moss was collected. Values for pH, humification degree, sulfur content (g/kg DW), organic matter, and water content of the studied moss, peat, gyttja, and clay layers and bog water samples were determined previously [80,104,106] (Table 1). X-ray diffraction analysis for the mineral gyttja and clay layer samples was performed to examine the presence of clay minerals as described previously in [80] (Table 1).

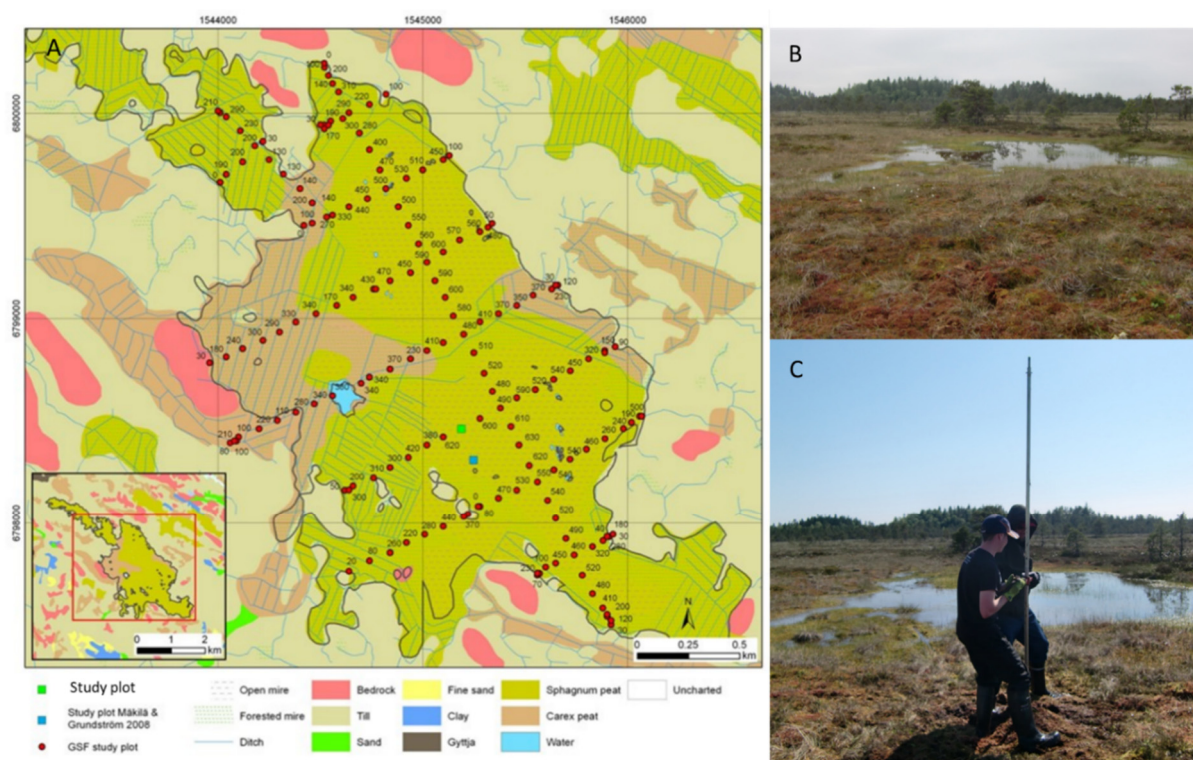


Figure 1. (A) Map of Lastensuo bog, (B) sampling point in the center of the bog, and (C) sampling with a peat corer.

Table 1. pH of bog water and bog layer, humification degree (%), organic matter content (%), water content (%), and number of bacterial 16S rRNA genes g^{-1} DW of the bog samples from Lastensuo bog [80,106]. S concentrations (g/kg DW) were calculated as average concentrations obtained from the data of Aro et al. [104]. Data for mineral fractions and exchangeable cations (meq/100 g) from 1 M ammonium acetate extractions as well as the sum of extractable cations (meq/100 g) were obtained from in [38,80]. ND = no determination.

Sample	Bog Water pH	Bog Layer pH	Humification Degree	Organic Matter	Water Content	Number of Bacterial 16S rRNA Genes	S Content g/kg DW
Surface moss	3.8	3.1	H1	99.2	92.0	5.0×10^{10}	1.7
Peat 0.5 m	4.7	3.1	H3	99.5	88.8	5.0×10^{10}	1.3
Peat 1.5 m	ND	3.1	H4	99.6	90.9	1.0×10^{10}	2.7
Peat 2.5 m	4.9	3.2	H4	99.8	66.2	2.0×10^9	2.4
Peat 3.5 m	ND	3.2	H4/H5	99.8	94.1	1.0×10^{10}	2.4
Peat 3.7 m	ND	3.3	H5	99.8	91.0	1.0×10^{10}	ND
Gyttja 5.5 m	5.2	4.0	H6	95.0	83.3	1.0×10^{10}	1.2
Clay 6.5 m	ND	5.3	Clay	15.3	73.2	5.0×10^9	17.3
	Na NH ₄ AC	K NH ₄ AC	Ca NH ₄ AC	Mg NH ₄ AC	Al NH ₄ AC	Sum (K ⁺ , Ca ²⁺ , Mg ²⁺ , Na ⁺ , Al ³⁺)	
Surface moss	1.1	4.4	2.6	3.4	1.5	13	
Peat 0.5 m	0.2	0.3	1.0	3.0	1.1	6	
Peat 1.5 m	0.2	0.2	1.8	3.4	0.6	6	
Peat 2.5 m	0.3	0.4	2.5	4.3	0.5	8	
Peat 3.5 m	0.4	0.2	2.8	7.0	0.4	11	
Peat 3.7 m	0.3	0.2	5.6	9.1	0.5	16	
Gyttja 5.5 m	0.2	0.3	18.7	11.8	6.2	37	
Clay 6.5 m	ND	ND	ND	ND	ND	ND	
Minerals in <2 μm fraction				Minerals in >2 μm fraction			
Gyttja and Clay	Illite, clinochlore and kaolinite			Quartz, microcline, plagioclase, pyrite, Fe-hornblende			

2.2. Nucleic Acid Isolation

Microbial community DNA was isolated from two parallel samples, A and B, of approximately 0.5 g subsamples of thawed surface moss, peat, gyttja, and clay samples with a NucleoSpin® Soil DNA extraction kit (MACHEREY-NAGEL GmbH & Co. KG, Dürren, Germany). Sample types with different characteristics, such as high content of organic material, high mineral content, varying pH, etc., may require dissimilar lysis conditions for optimal results. In order to increase the possibility to lyse as many different types of microbial cells as possible and detect the widest microbial diversity, the replicate samples were treated with different lysis buffers provided in the DNA extraction kit. Sample A was extracted with Lysis Buffer SL1 and sample B with Lysis Buffer 2. Enhancer solution SE was used with both samples and the extraction proceeded according to the manufacturer's instructions. Negative DNA isolation controls were included in the isolation protocol. The DNA was eluted in 100 µL elution buffer and the DNA concentration of each extract was measured using the NanoDrop-1000 spectrophotometer (Thermo Fisher Scientific, Waltham, MA, USA).

2.3. Amplicon Library Preparation

The bacterial community was studied by high-throughput amplicon sequencing using the 454 Titanium FLX technology (Roche) and was previously reported [106]. The data were re-analyzed here and combined with the fungal and archaeal data. The archaeal and fungal communities were analyzed with high-throughput sequencing of the archaeal v4 region of the 16S rRNA gene and fungal internal transcribed spacer 1 (ITS1) region using the Ion Torrent PGM platform previously described [107]. The archaeal primers were the S-D-Arch-0349-a-S-17 (5'- GYGCASCAGKCGMGAAG-3') and S-D-Arch-0787-a-A-20 (5'- GGACTACVSGGGTATCTAAT -3') [108] and the fungal primers the ITS1 (5'- CTTGGTCATTAGAGGAAGTA-3') and ITS2 (5'- GCTGCGTTCTTCATCGATGC-3') [109,110]. Primers 8F (5'- AGAGTTTGATCCTGGCTCAG-3') and P2 (5'- CAG GCC TAA CAC ATG CAA GTC-3') were used for amplifying the v1–v3 region of the bacterial 16S rRNA gene [111,112].

2.4. Sequence Processing and Analysis

The sequence reads were analyzed using the Mothur software (v.1.43.0) [113] as earlier described [107]. The archaeal and bacterial 16S rRNA sequences were aligned to the Silva version 138 reference alignment [114,115] using Mothur. The fungal ITS1 sequences were identified using the dynamic version of the UNITE ITS data base version 6 [116–118], as previously described [107]. Sequence reads were clustered into operational taxonomic units (OTUs) sharing 97% identity. For comparing alpha diversity metrics the fungal ITS and for bacterial 16S rRNA gene sequence data sets were normalized to a subset of 2000 random sequences for sequences per sample and 1000 sequences per sample for the archaea. The alpha diversity analyses included the Shannon diversity indices and the estimated Chao1 OTU richness.

The bacterial sequences have previously been deposited to the European Nucleotide Archive (ENA, <http://www.ebi.ac.uk/ena>) under Study accession number PRJEB6875. The archaeal and fungal sequences have been submitted to the ENA under Study accession number PRJEB41440.

2.5. Sorption Batch Experiments Data and Metal Concentrations

Ni, Ag, Se, I, and Cs sorption data were obtained as previously described [119]. Briefly, batch sorption experiments were used to determine the distribution coefficients (K_d) of subsurface peat, gyttja, and clay. The experiments were set up aseptically by mixing 0.5 g of fresh sample and 25 mL of sterilized artificial bog water (see in [119]) and incubating for one week in order for the cation and anion concentrations to stabilize. The stabilization was confirmed by inductively coupled plasma mass spectrometry (ICP-MS) (Agilent 7500ce, Agilent Technologies, Inc., Santa Clara, CA, USA) measurement of the cations in the model

bog water solution. After this, the tracers of ^{63}Ni , $^{110\text{m}}\text{Ag}$, ^{134}Cs , ^{125}I , and ^{75}Se were added with activities of 200 Bq per sample for ^{63}Ni , $^{110\text{m}}\text{Ag}$, ^{125}I , and ^{75}Se . For ^{134}Cs 1000 Bq per sample was used. Incubation of the samples was continued at 20 °C for 7 days under constant mixing. Thereafter, the samples were submitted to a 20 min centrifugation at 20,000 rpm (Beckman Coulter J-26 XPI, rotor JA-25.50), filtered through a 0.2 µm syringe filter, the filtrate pH was measured whereafter the filtered solution was used for gamma spectrometric determination of ^{63}Ni , $^{110\text{m}}\text{Ag}$, ^{75}Se , ^{125}I and ^{134}Cs activity as previously described [119]. The batch K_d values of the experiment were calculated as previously described [119]. Three parallel samples were used for all measurements. Batch sorption data for Se, I, and anoxic Se and I were obtained from our previous studies [80,119] (Table 2). For the anoxic determinations, only the innermost parts of the peat corer nest samples were used and transferred tightly sealed in plastic from the sampling site into a nitrogen cabinet [119]. The samples were further handled as described above, except under anoxic conditions. The redox potential (Eh (V)) was recorded for the redox sensitive species at the end of the incubation period.

Table 2. Geometrical mean of sorption data (K_d values L/kg DW, three replicate samples) for Ni, Ag, and Cs (this paper), and Se, I, anoxic Se, and anoxic I (data from in [80,119]) after 7 days of incubation at 20 °C.

Sample	Ni	Ag	Cs	Se	I	Se Anoxic *	I Anoxic *
Surface moss	nd	nd	93	4388	1797	nd	nd
Peat 0.5 m	11,727	21,743	115	2602	478	15	226
Peat 2.5 m	7817	21,783	113	2716	80	18	194
Gyttja 5.5 m	19,880	17,778	221	696	316	6	1629
Clay 6.5 m	190	10,699	1601	735	24	0	333

* geometrical mean of two replicate samples; nd—no data.

Microwave-assisted HNO_3 extraction was used to determine the overall sodium (Na), magnesium (Mg), aluminium (Al), potassium (K), calcium (Ca), iron (Fe), cobalt (Co), Ni, copper (Cu), zinc (Zn), Se, molybdenum (Mo), silver (Ag), cesium (Cs), thorium (Th), and uranium (U) concentrations in the surface moss, peat, gyttja, and bottom clay samples. A 0.5 g subsample of fresh soil was weighed into a Teflon tube to which 10 mL HNO_3 (concentrated) was added, and the sample was wet digested in a microwave oven using the EPA3051 method (Milestone Inc., Shelton, CT, USA). The extract solutions were filtered through a 0.2 µm Supor membrane filter (Pall Corp., Port Washington, NY, USA), the samples were diluted to 1:33, and the metal concentrations were determined using ICP-MS (Agilent 7500ce, Agilent Technologies, Inc., Santa Clara, CA, USA). No-sample negative control samples, containing only extraction solutions, were used in the extractions to detect possible reagent contamination. All ICP-MS determinations were performed using two parallel samples, and control samples with known concentrations were included in all ICP-MS runs. The microwave-assisted conc. HNO_3 extraction was able to totally dissolve the organic peat layer fractions, but for the lowest mineral clay layer a small proportion of siliceous residue remained after digestion. This was removed in the following filtration step. Unlike sequential extractions, HNO_3 extraction does not distinguish between exchangeable fraction, metals bound on oxide minerals (Fe(III)), organics, or primary sulfides.

2.6. Statistical Analyses

The relationships between the measured metal concentrations and Ni, Ag, Cs, Se, and I sorption data and microbial communities were examined with univariate analysis (Pearson's r). The relationships between pH, water content, and humification degree versus bacterial, archaeal, and fungal communities; community richness (Chao 1); and diversity (Shannon index H') of the bacterial, archaeal, and fungal communities were also examined using univariate analysis (Pearson's r) with all samples and separately with only peat samples. In addition, the correlation between number of bacteria (as number of bacterial 16S rRNA gene copies g^{-1} dry weight sample) reported by Tsitko et al. [106] and sorption

of radionuclides and metal concentrations was tested. All comparisons were Bonferroni corrected in order to minimize false positive correlations. The normal distribution of the data was evaluated by the Shapiro–Wilk test ($p < 0.05$) before the analysis. The normality hypothesis was rejected for all used data. All statistical analyses were performed using PAST v. 4 [120]. The statistical analyses were performed on the genus rank. Only groups with relative abundances of $> 0.1\%$ in at least one of the studied bog layers were included in the analyses. The differences in the microbial communities of the different bog layers were analyzed with Principal Coordinates Analysis (PCoA) using Phyloseq in R [121,122]. The PCoA were performed on the relative abundance of OTUs, including only samples with at least 1000 sequence reads, using the Bray–Curtis distance model. The statistical significance of environmental parameters on the distribution of samples on the PCoA chart was tested with 999 permutations and parameters with $p < 0.05$ were plotted as vectors on the plots.

3. Results

3.1. Sorption Experiments

The sorption (reported as K_d values liters (L) per dry weight kg (DW)) of Ni in all studied bog samples was found somewhat lower than the corresponding K_d values for Ag after one week stabilization period (Table 2, Figure 2A). Ni K_d values varied from 190 L/kg DW detected in the clay layer to 19,900 L/kg DW in the gyttja layer after one week equilibrium time. Ag K_d values ranged from 10,000 L/kg DW to 33,400 L/kg DW, with the highest values recorded for the peat layer from 2.5 m depth. Cs K_d values were found several orders of magnitude lower than those observed for Ag and Ni. Highest values (1600 L/kg DW) were observed for the clay layer (Figure 2B).

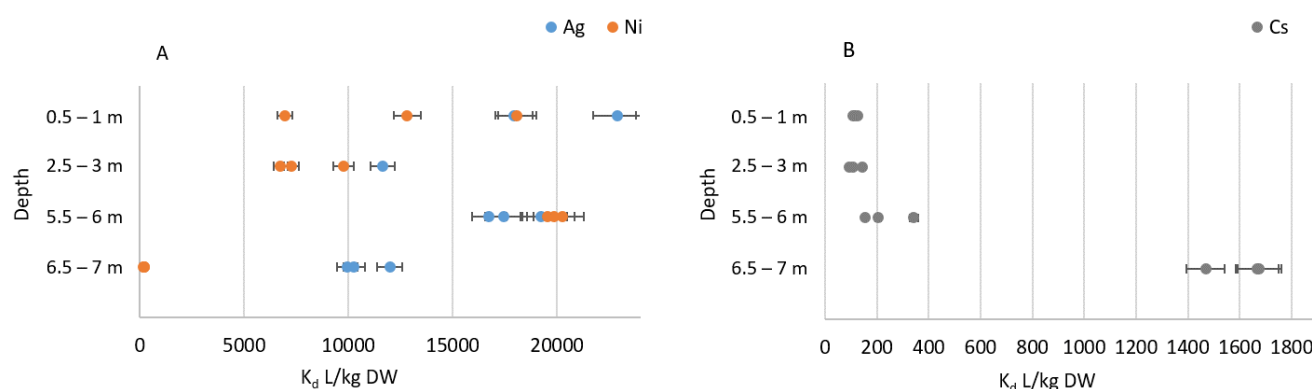


Figure 2. Ag, Ni (A) and Cs (B) K_d values (L/kg DW) in fresh Lastensuo bog samples from 0.5–1 to 6.5–7 m. Layers from 0.5 m to 3.0 m consisted of peat, layer 5.5 m of gyttja, and layer 6.5 m of clay. Error bars indicate 5% measurement uncertainty. The figure shows all three parallel samples.

In comparison, the sorption values for Se and I (reported in [80,119]) were 696–4388 L/kg and 24–1797 L/kg, respectively, in the aerobic incubations and 0–18 L/kg and 194–1629 L/kg, respectively, in the anaerobic incubations (Table 2). The recorded average Eh values for 0.5 m peat, 2.5 m peat, 5.5 m gyttja, and 6.5 m clay layers were 0.40 ± 0.05 V, 0.41 ± 0.06 V, 0.29 ± 0.08 V, and 0.12 ± 0.06 V, respectively, indicating more reducing conditions at the lower layers, compared to the upper layers.

3.2. Metal Concentrations

The metal concentrations varied between different bog layers and for all samples, and the highest concentration of metals was found in the lowest clay layer (Table 3). In addition, high concentrations of Na, Mg, Al, K, and Ca were found in the surface moss, 433 mg/kg DW, 634 mg/kg DW, 273 mg/kg DW, 4673 mg/kg DW, and 1619 mg/kg DW, respectively. Naturally occurring Ni, Ag, Cs, Se, and Th were generally detected at low concentrations,

or not at all. With the exception of Ag, the highest concentrations were found in the clay layer (Table 3). Ni was also detected in the peat layers at 0.5 m and 1.5 m. Th was also detected in the gyttja layer.

Table 3. Metal concentrations from the microwave assistant extraction of Lastensuo bog surface moss, peat, gyttja, and clay layers (mg/kg DW).

	Surface	0.5 m	1.5 m	2.5 m	3.5 m	5.5 m	6.5 m
Na	433	0	0	0	202	0	430
Mg	634	687	581	831	2410	1520	6562
Al	273	350	221	197	650	>1486	>1486
K	4673	344	186	319	241	271	6156
Ca	1619	1193	955	938	2566	4030	4124
Fe	423	522	401	271	558	1509	25,543
Co	0.04	0.03	0.04	0.02	0.02	1.01	11
Ni	0	20	15	0	0	0	34
Cu	13	5.01	3.02	0	1.04	25	35
Zn	48	37	23	19	21	23	90
Se	0	0	0	0	0	0	6.05
Mo	0.03	4.00	4.00	0	0	0.09	6.02
Ag	0.02	0.02	0.01	0.02	0.01	0.01	0.02
Cs	0.05	0.01	0.01	0	0.01	0.01	3.03
Th	0.01	0.01	0.01	0	0.01	1.03	7.06
U	0	0	0	0	0	1.01	4.04

3.3. Archaeal, Fungal, and Bacterial Diversity

A total of 1617 archaeal 16S rRNA genes and 1670 fungal ITS1 Operational Taxonomic Units (OTUs) were identified from the amplicon sequence data, when clustered at 97% sequence homology. The bacterial 16S rRNA gene sequence data from [106] were reanalyzed and contained a total of 5029 bacterial OTUs. The highest number of 293 identified and 513 Chao1 estimated average number archaeal OTUs in the rarefied data was obtained from the surface moss sample (Table 4). The highest archaeal diversity index (H' (average) = 4.8) was also seen in the surface moss. The lowest average number of identified (129) and estimated archaeal OTUs (294) was observed in the peat sample from 3.7 m. The lowest Shannon diversity index (H' (average) = 1.6) was detected in the peat from 0.5–1.0 m depth. For all peat layer samples from 0.5 m to 3.7 m the number of observed and Chao1 estimated OTUs was below 150 and 180, respectively (Table 2). In the lowest clay layer (6.5 m), the number of archaeal OTUs was higher compared to the peat layers, with on average 198 observed and up to 314 Chao1 estimated archaeal OTUs.

The highest average number of fungal ITS OTUs in the rarefied data was observed in the peat from 0.5 m (Table 5), with an average of 297 identified and 323 Chao1 estimated fungal OTUs. The highest fungal diversity index (H' (average) = 3.8) was found in the surface moss and the lowest (H' (average) = 2.8) in the bog middle layers from 2.5 m to 3.5 m, where also the lowest average number of identified (160) and estimated fungal OTUs (256) were detected. The mean number of fungal OTUs and Chao1 estimated OTUs in the clay layer was 276 and 303, respectively, with a mean H' of 3.2.

The highest number of rarefied bacterial OTUs and Chao1 estimated OTUs was observed in the peat layer from 1.5 m (Table 6). The surface moss has the highest Shannon's H' of 5.5. The lowest number of identified (191) and Chao1 estimated OTUs (385) were observed in the peat sample from 2.5 m depth.

Table 4. The total number of archaeal 16S rRNA gene sequence reads (Sequences), and the number of observed (OTUs) and Chao1 estimated archaeal OTUs (Chao1), Good's coverage (%) of detected OTUs estimated from the Chao1 (Coverage), and Shannon's diversity indices (Shannon H') calculated from the rarefied (1000 sequence reads) data. Samples A and B are the duplicate samples from the same layer and the DNA was extracted using Extraction Buffer SL1 and SL2 for sample A and B, respectively.

Sample	Sequences	OTUs	Chao 1	Coverage (%)	Shannon H'
Surface A	1228	283	505	88	4.7
Surface B	1215	302	520	87	4.8
Peat 0.5 m A	12,587	145	311	99	1.7
Peat 0.5 m B	13,314	148	285	99	1.6
Peat 1.5 m A	11,034	128	204	99	2.2
Peat 1.5 m B	11,470	141	252	99	2.1
Peat 2.5 m A	2212	100	159	98	2.8
Peat 2.5 m B	5971	160	273	99	2.8
Peat 3.5 m A	9871	170	411	99	2.3
Peat 3.5 m B	11,672	129	263	99	2.1
Peat 3.7 m A	13,120	177	445	99	2.0
Peat 3.7 m B	4354	80	143	99	2.0
Gyttja 5.5 m A	23,698	280	493	99	2.4
Gyttja 5.5 m B	19,757	200	325	100	2.3
Clay 6.5 m A	18,925	200	314	100	1.9
Clay 6.5 m B	14,913	195	293	99	2.1

Table 5. Obtained number of fungal ITS1 region sequence reads (Sequences), observed (OTUs) and estimated (Chao1) number of fungal OTUs, Good's OTU coverage (%) estimated from the Chao1 (Coverage), and diversity index (Shannon H') calculated from the sequence data. The data were rarefied to 2000 sequences for calculating the number of OTUs, Shannon index, Chao1 estimate, and Good's coverage. The coverage describes the percentage of OTUs detected from the rarefied data set compared to the Chao1 estimated number of OTUs determined from the rarefied data. Samples A and B are the duplicate samples from the same layer and the DNA was extracted using Extraction Buffer SL1 and SL2 for sample A and B, respectively.

Sample	Sequences	OTUs	Chao 1	Coverage (%)	Shannon H'
Surface A	7067	323	418	99	3.8
Surface B	4495	237	343	98	3.7
Peat 0.5 m A	20,265	308	463	99	3.8
Peat 0.5 m B	17,543	286	379	99	3.1
Peat 1.5 m A	18,224	291	406	99	3.7
Peat 1.5 m B	17,433	209	307	100	3.1
Peat 2.5 m A	5689	120	171	99	2.7
Peat 2.5 m B	10,079	206	307	99	2.9
Peat 3.5 m A	7023	156	307	99	2.9
Peat 3.5 m B	8419	159	240	99	2.6
Peat 3.7 m A	14,233	327	465	99	3.4
Peat 3.7 m B	17,236	218	287	100	2.2
Gyttja 5.5 m A	13,782	259	445	99	2.9
Gyttja 5.5 m B	18,917	246	350	100	3.3
Clay 6.5 m A	13,924	241	388	99	3.2
Clay 6.5 m B	17,840	310	433	99	3.1

Table 6. Obtained number of bacterial 16S rRNA gene sequence reads (Sequences), observed (OTUs) and estimated (Chao1) number of bacterial OTUs, Good's OTU coverage (%) estimated from the Chao1 (Coverage), and diversity index (Shannon) of the communities. The data were rarefied to 2000 sequences for calculating the number of OTUs, Shannon index, Chao1 estimate, and Good's coverage. The coverage describes the percentage of OTUs detected from the rarefied data set compared to the Chao1 estimated number of OTUs determined from the rarefied data. Samples A and B are the duplicate samples from the same layer and the DNA was extracted using Extraction Buffer SL1 and SL2 for sample A and B, respectively.

Sample	Sequences	OTUs	Chao 1	Coverage (%)	Shannon H'
Surface A	3089	654	1348	88	5.5
Surface B	7988	1063	2015	93	5.5
Peat 0.5 m A	2961	546	1365	88	4.6
Peat 0.5 m B	9295	697	1422	96	4.1
Peat 1.5 m A	36,102	1122	2420	98	3.3
Peat 1.5 m B	8723	321	603	98	2.9
Peat 2.5 m A	7937	382	812	97	3.6
Peat 2.5 m B	15,327	634	1376	98	3.7
Peat 3.5 m *	3841	191	385	97	3.4
Peat 3.7 m *	5256	261	410	98	2.9
Gyttja 5.5 m A	5992	556	1196	95	4.4
Gyttja 5.5 m B	9743	731	1393	96	4.3
Clay 6.5 m A	2811	575	1502	87	5.1
Clay 6.5 m B	5002	633	1142	93	4.7

* No sequences were obtained from the B samples from peat 3.5 m and peat 3.7 m.

3.4. Archaeal, Fungal, and Bacterial Community Compositions

The archaeal community in the Lastensuo bog depth profile, contained a total of 37 different genera belonging to 10 archaeal phyla. The major part of the community affiliated with the *Crenarchaeota*, *Halobacterota*, and *Thermoplasmatota* (Figure 3). *Crenarchaeota* dominated the archaeal community especially in the lower peat, gyttja, and clay layers from 2.5 m to 6.5 m (45–83% of sequence reads). Archaea remaining without classification (unclassified archaeota) were clearly most common in the surface moss layer (on average 85% of sequence reads). The relative abundance of *Halobacterota* and *Thermoplasmatota* decreased with depth, the highest relative abundance observed in the 0.5 m peat layer (43% and 41% of sequence reads, respectively).

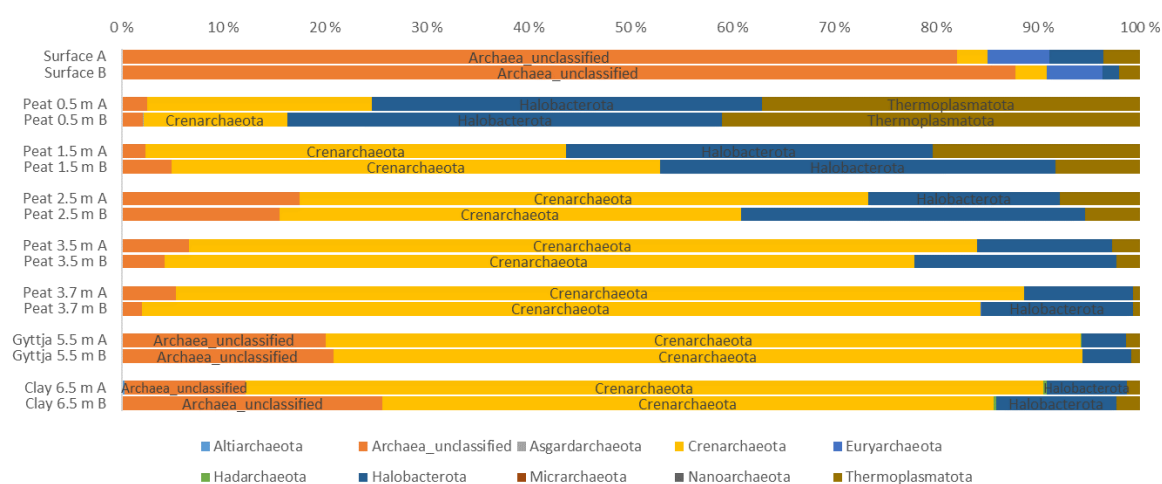


Figure 3. Relative distribution of archaeal phyla in surface moss, peat, gyttja and clay samples collected from Lastensuo bog. Each depth is represented by duplicate samples A and B.

Candidatus Altiarchaeum, *Nitrososphaeria* (Marine Benthic Group A), *Methanomicrobiaceae* (uncultured), and unclassified *Methanomicrobiales* were only found in the lowest clay sample (6.5 m) (Figure A1), whereas *Bathyarchaeia* contributed with on average 68% of sequence reads. The clay layer contained the highest number (19) of archaeal genera (Figure A1), whereas the lowest number of eight archaeal genera was found in the surface layer (unclassified archaea, *Bathyarchaeia*, *Nitrososphaeria* Group 1.1c, unclassified *Methanobacteriaceae*, *Methanobacterium*, *Methanomicrobiales* Rice Cluster II, *Methanomassiliicoccus*, unclassified *Thermoplasmata*). In the surface moss layer, 85% of archaeal sequence reads consisted of unclassified archaeota. Unclassified *Nitrososphaeria* was the most common archaeal lineage in the 5.5 m gyttja layer with 35% of sequences belonging to this genus.

Five fungal phyla (Figure 4), representing 145 different genera (Figure A2), were found throughout the Lastensuo Bog profile. Ascomycota generally dominated the fungal communities, with the exception of the surface moss, where unclassified fungi dominated with relative abundances >50%. *Basidiomycota* were most commonly found in the surface moss sample, representing on average 13% of the fungal community, and were less common in the deeper layers. In the peat, gyttja, and clay layers, *Ascomycota* formed 77–78% of the fungal population.

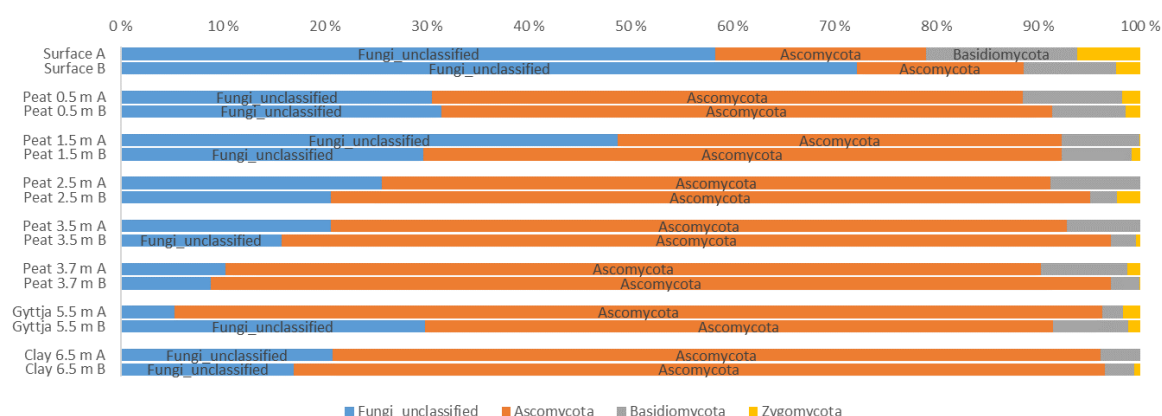


Figure 4. Relative distribution of fungal phyla in surface moss, peat, gyttja, and clay samples collected from Lastensuo bog. Each depth is represented by duplicate samples A and B.

Of the detected genera (Figure A2), *Phaeoacremonium* formed 37% of the fungal community in the Lastensuo Bog, whereas 26% of the sequence reads on genus level belonged to unclassified fungi. The highest mean relative abundance of *Phaeoacremonium* (53%) was observed in the clay layer.

Acidobacteriota, *Proteobacteria*, and *Chloroflexi* were the most common bacterial taxa in the bog samples (Figure 5, Figure A3). *Spirochaetota* were found especially in the lowest gyttja (5.5 m) and clay (6.5 m) layers. *Acidobacteriota* covered 21–87% of the sequence reads of each sample, with the lowest numbers in the clay. *Proteobacteria* were common in the surface moss samples, contributing with 41% of the bacterial 16S rRNA gene sequence reads. *Chloroflexi* covered 35% of bacterial community in the 3.7 m peat layer. *Spirochaetota* contributed with 17% of the bacterial community in the clay layer (6.5 m). Other bacterial phyla detected in the bog samples included, e.g., *Planctomycetota* (11% in the 6.5 m clay layer) and *Actinobacteria* (6.3%, 2.7% and 2.2% in the 3.5 m and 3.7 m peat and surface moss layer, respectively). In the clay layer, 11% of the bacterial sequence reads remained without further classification.

A total of 333 bacterial genera were identified from the whole bog profile. *Acidobacteriota* were represented by 33 genera. The most prominent genus belonged to *Acidobacteriaceae* Subgroup 13 (Figure A4), which was most common in the 1.5 m peat sample covering a mean 64% of the bacterial community. *Granulicella* (14%) and *Candidatus Solibacter* (12%) were observed especially in the 2.5 m peat sample. The clay layer bacterial community

contained 6.3% *Aminicenantales*, whereas the surface layer was colonized by *Occallatibacter* (9.0%) and uncultured *Acidobacteriales* (8.4%).

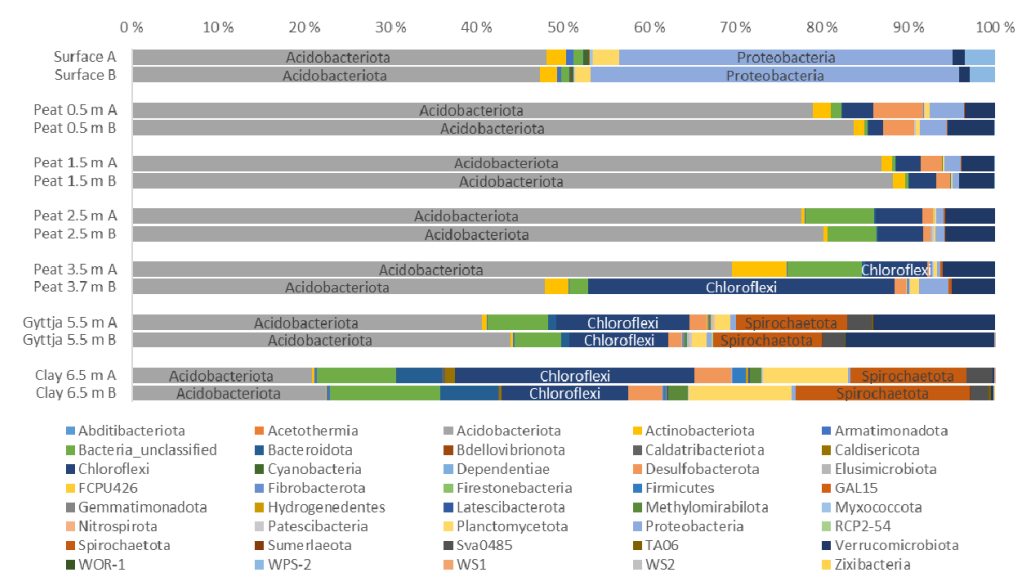


Figure 5. Relative distribution of bacterial phyla in surface moss, peat, gyttja, and clay samples collected from Lastensuo Bog. Each depth is represented by duplicate samples A and B.

Proteobacteria were represented mainly by Alphaproteobacteria (75% of the Proteobacteria) (Figure A5) and Gammaproteobacteria (25% of the proteobacteria, Figure A6). In the surface moss, alphaproteobacterial contributed with 19% of the bacterial community, of which *Roseiarcus* and a genus belonging to uncultured *Acetobacteraceae* contributed with 4.9% and 3.5% of the bacterial sequence reads, respectively. In all peat layers from 0.5 m to 3.5 m, uncultured *Acetobacteraceae* dominated the alphaproteobacterial community. In the gyttja and clay layers alphaproteobacterial represented less than 0.1% of the bacterial communities.

Gammaproteobacteria were most commonly found in the surface moss (~6.5% of all sequence reads). The gammaproteobacterial sequence reads were mostly assigned to the WD260 group (6.6% in total in all samples), unclassified *Burkholderiales* (in total 2.1%), and *Acidibacter* (in total 1.6%). The relative abundance of all other observed gammaproteobacterial genera was <1%.

Chloroflexi were most common in the peat layer from 3.7 m, where they contributed with 35% of the sequence reads. The most prominent genus, covering 99% of the *Chloroflexi*, was the *Dehalococcoidia* GIF9 (Figure A7). In all other peat layers, *Chloroflexi* contributed with <8% of the bacterial sequence reads and were not found in the surface layer. In contrast, the gyttja and clay layers contained several *Chloroflexi* genera, with *Dehalococcoidia* GIF9 contributing with 31% of the bacterial community of the gyttja and *Dehalococcoidia* SCGC-AB-539-J10 and unclassified *Dehalococcoidia*, together contributing with 43% the bacterial community in the clay layer.

Spirochaetota were represented by four groups, i.e., the *Brevinema*, *Spirochaeta*, unclassified *Spirochaetaceae*, and uncultured *Spirochaetaceae*, the most prominent group being *Spirochaeta* which covered 99.9% of all *Spirochaetota* reads. *Spirochaetota* were mainly found in the lowest gyttja and clay layers, with low abundances, covering on average 3.9 % of all bacterial sequence reads.

3.5. Correlation between Microbial Communities, Alpha diversity, and Physicochemical Parameters

No correlations between archaeal genera or archaeal out numbers, Chao1 richness, or Shannon's H' and sorption data or between fungal OTU numbers, Chao1 richness, or H' index and metal concentrations or bog characteristics data (pH, etc.) were found. However, several archaeal genera showed positive correlation (based on Bonferroni-corrected

p -values) with pH, Eh, and different metal concentrations (Table A1). *Lokiarchaeia*, *Hadarchaeales*, uncultured *Methanomicrobiaceae*, *Methanosaeta*, and uncultured *Methanomassiliicoccaceae* showed strong positive correlation to pH ($p < 0.05$ – 0.00001), whereas *Lokiarchaeia* correlated negatively ($p < 0.05$) to Eh). An unclassified crenarchaeotal genus correlated positively to the humification degree ($p < 0.05$). Interestingly, *Hadarchaeales*, uncultured *Methanomicrobiaceae*, *Methanosaeta*, and uncultured *Methanomassiliicoccaceae* correlated negatively with the amount of organic matter in the samples ($p < 0.05$ – 0.00001). *Candidatus Altiarchaeum*, *Lokiarchaeia*, *Hadarchaeales*, uncultured *Methanomicrobiaceae*, *Methanosaeta*, and uncultured *Methanomassiliicoccaceae* correlated positively with concentrations of Fe, Co, Se, Cs, Th, and U. *Lokiarchaeia*, *Hadarchaeales*, uncultured *Methanomicrobiaceae*, *Methanosaeta*, and uncultured *Methanomassiliicoccaceae* correlated positively with Mg. In addition, *Lokiarchaeia* and *Methanosaeta* correlated positively with Cu and *Hadarchaeales* and uncultured *Methanomicrobiaceae* with Zn. The presence of *Lokiarchaeia* and *Methanosaeta* correlated negatively with Ag sorption (K_d values) in the Lastensuo bog samples, whereas *Hadarchaeales* correlated positively with Cs sorption (Table 7).

Table 7. Pearson correlation coefficients of the Bonferroni corrected correlations between relative abundance of bacterial genera or bacterial numbers and sorption data. Correlation coefficients for pairs with $p < 0.05$ are shown.

	Ag Sorption	Cs Sorption	Se Sorption	Se Anoxic Sorption	I Anoxic Sorption
Lokiarchaeia genus	−0.98				
Methanosaeta	−0.98				
Hadarchaeales genus		0.98			
Acetothermii_ge		1.0			
GOUTB8_ge		1.0			
Thermoanaerobaculum		1.0			
Pelolinea		1.0			
Anaerolineaceae;uncultured					0.99
Latescibacteraceae_unclassified		1.0			
MidBa8_ge		1.0			
DG-20_ge		1.0			
Bacterial number			0.99 ***	0.96	

*** $p < 0.00001$.

No statistically significant correlations were observed between fungal genera and pH, water content, humification degree, depth, organic matter content, nor metal concentrations. Neither were correlations between fungal genera or fungal OTU numbers, Chao1 richness, or Shannon's H' and sorption data found.

The metal concentrations found in the bog samples did not correlate significantly with the number of bacterial 16S rRNA genes, OTUs, Shannon's diversity index (H'), or Chao1 richness. However, several strong positive correlations between bacterial genera (Table A2) and metal concentrations were observed. The strongest positive correlations were observed between *Pelolinea* and *Phycisphaerae* DG-20 and Fe, Se, and Cs ($r > 0.999$, $p < 0.05$). Strong positive correlations ($r \geq 0.997$) were in addition observed between several other bacterial genera (e.g., *Acetothermii*, *Lateibacteraceae*, *Polyangia*, and *Phycisphaerae*) and Fe, Co, Se, and Cs (Table A2).

Strong positive correlations ($r \geq 0.995$, $p < 0.01$) between bacterial genera and Cs sorption (K_d values) were observed (Table 7). The bacteria with strong positive correlations with Cs sorption data included *Aceothermii*, *Acidobacteriae* GOUTB8, *Thermoanaerobaculum*, *Pelolinea*, *Latescibacteraceae*, *Polyangia* MidBa8, and *Phycisphaerae*. In addition, anoxic sorption data for Se correlated positively ($r = 0.993$, $p = 0.04$) with uncultured *Anaerolineaceae*. No correlations between any of the other sorption data (I, Se, Ni, and Ag) and bacterial genera were found.

Several bacterial genera correlated with organic matter content (%) (Table A2). All of the statistically significant correlations were negative and included, e.g., *Aceothermii*,

Acidobacteriae GOUTB8, *Thermoanaerobaculum*, *Pelolinea*, *Latescibacteraceae*, *Polyangia* MidBa8, and *Phycisphaerae* (Table A2).

The similarity between the archaeal, fungal, and bacterial communities of the different bog layers was tested using Principal Coordinates analysis (PCoA) and the Bray–Curtis dissimilarity model (Figure 6). For all microbial groups, the surface samples separated from the rest of the samples. The archaeal community in the surface samples (the highest relative abundance of unclassified archaea) appeared to be affected by the concentration of Ag, whereas the fungal and bacterial communities of the same sample were not (Figure 6A). The archaeal communities of the peat samples also clearly clustered according to depth, with samples from similar depths falling closer together. The gyttja and clay communities were clearly different from the surface and peat communities, and although not clustering together, both sample types fell in the upper left quadrant of the plot where the metal concentrations had the highest influence. In the fungal PCoA analysis, the surfaces samples separated to the opposite side of the plot from the rest of the samples (Figure 6B). All peat, gyttja, and clay samples fell to the right side of the plot and did not clearly separate from each other. No environmental parameters appeared to affect the fungal communities with any statistical significance. The bacterial communities separated into three distinct groups: the surface communities, the peat and gyttja communities, and the clay communities. The clay community was most strongly affected by the measured metals.

No statistically significant correlation between bacterial numbers or microbial taxa and the concentration of Ni or Ag, or sorption of Ni and Ag in the tested samples, was seen. In the regression analysis, the sorption of Ni did not appear to be affected by bacterial numbers or by sample type. However, the higher sorption of Ag was seen in the samples with the highest number of bacteria, and lowest in the clay sample, with the lowest number of bacteria and generally different conditions compared to peat (Figure 7A,B).

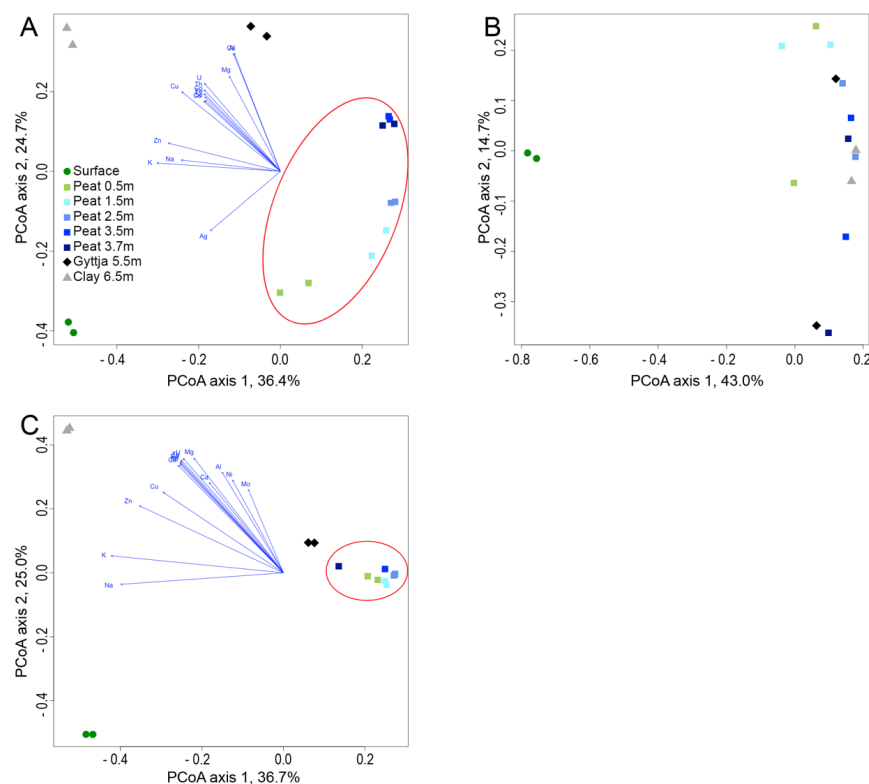


Figure 6. Principal Coordinates Analysis (PCoA) of the (A) archaeal, (B) fungal, and (C) bacterial communities in relation to environmental parameters. Vectors for metal concentrations having statistically significant ($p < 0.05$) effect on the microbial communities are shown. For fungi, no significant metal concentrations were identified. In A and C, the peat samples are indicated with a red oval.

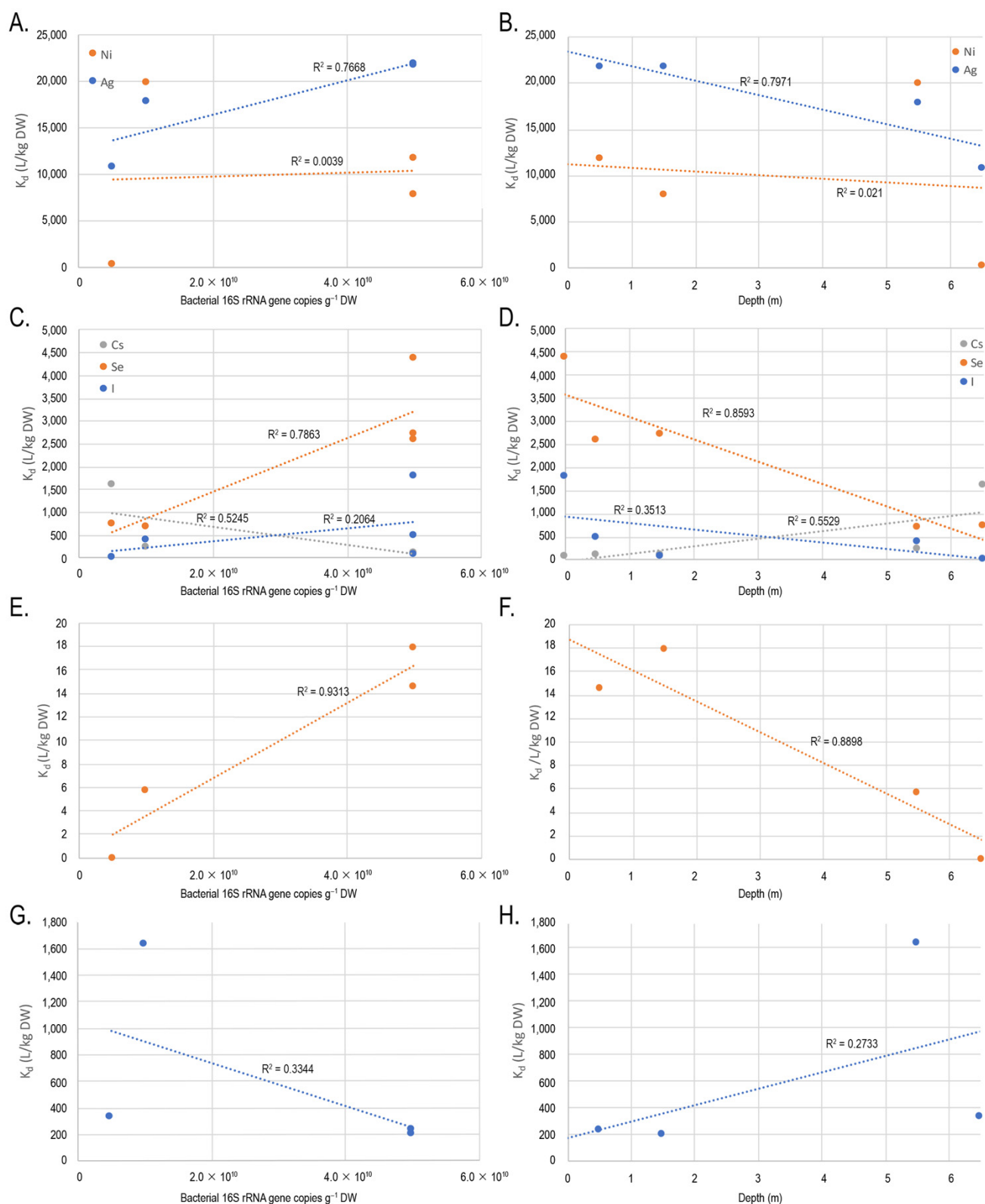


Figure 7. The sorption (K_d) of (A,B) Ni and Ag; (C,D) Cs, Se, and Ag; (E,F) anoxic Se; and (G,H) anoxic I plotted against (A,C,E,G) bacterial numbers (16S rRNA gene copies g^{-1} DW) and (B,D,F,H) sampling depth, i.e., sample type.

The concentration and sorption of Cs correlated strongly with several microbial groups (Tables 7, A1 and A2), but not with the number of bacterial 16S rRNA gene copies. The regression analysis is in agreement with these results, showing highest sorption of Cs in the

clay layer (Figure 7D). In contrast, the sorption of Se correlated strongly and significantly with the number of bacterial 16S rRNA genes (Table 7) under oxic ($p < 0.00001$) and anoxic ($p < 0.05$) conditions, which is also shown by the regression analysis, where the highest K_d values for Se coincides with the highest bacterial numbers (Figure 7). The sorption of I did not show statistically significant correlation with any microbial groups or bacterial numbers under aerobic conditions, but the regression analysis indicated slightly higher K_d values in samples with high bacterial counts, and lower K_d values in the clay layer. The sorption of I in anoxic conditions was low and now correlation with the bacterial numbers was seen (Table 7). However, uncultured *Anaerolineaceae* correlated positively with anaerobic iodine sorption (Table 7).

4. Discussion

Microbiological processes may affect the solubility and bioavailability of heavy metals and radionuclides, and consequently affect the overall behavior of these elements in the biosphere. Simultaneously, heavy metals and radionuclides and low pH, typical for ombrotrophic boreal bog environments, can select for microbial communities of more resilient types able to survive in these acidic and nutrient-poor environments [38,58,80]. In the present study, several factors, including variable metal concentrations, pH, organic matter content, humification degree, and bacterial numbers, were shown to influence the microbial community composition and/or vice versa in the acidic bog environment with high diversity of bacteria, archaea, and fungi (Tables 1 and 4, Table 5, Table 6). In addition, specific parts of the microbial communities were observed to correlate with radioactive Se, Cs, and Ag sorption behavior, as well as retention of I under anoxic conditions, which has also been reported earlier [40,46,65].

The alkali and heavy metal concentrations varied depending on the bog layer. However, the concentrations of, e.g., Cu, Pb, and Ni were not different from concentrations measured from four other Finnish oligotrophic bogs to a depth of 80 cm, but the concentration of Zn was elevated [2]. For all alkali and heavy metals, the highest concentrations were found in the bottom clay layer (Table 3), which was formed during the post-glacial land uplift in this area and once was part of the upper seabed [9]. High concentrations of alkali metals were also found especially in the surface moss sample and at the depth of 3.5 m in the peat. This ombrotrophic region is assumed to obtain all its nutrients through rainfall [9], which may explain the high alkali metal concentrations in the upper layers, from where they gradually diffuse through the peat layers eventually ending up to the lowest gyttja and clay layers. Interestingly, the highest H' values of the archaeal, fungal, and bacterial communities were observed in the surface moss layer with high alkali metal concentrations, which all are important nutrients. Heavy metals from the acid digestion including Fe, Co, and Se were concentrated in the bottom clay layer and several statistically significant positive correlations between archaeal and bacterial genera and these metals were found. Especially high positive correlations were also found between radionuclides U and Th, which are part of the natural decay series of uranium and were clearly concentrated to the bottom clay layer.

Ni was found at 0.5–1.5 m depth in the peat samples and in the clay layer at concentrations of 15–34 mg kg⁻¹ DW (Table Metals), and below the detection limit of the assay in the other samples. Ni is a key component in a functioning methyl-coenzyme M reductase (MCR) of methanogens [123], but no methanogenic archaea correlated with the Ni concentrations in Lastensuo. Many plant growth-promoting bacteria have the capacity to reduce the toxicity of Ni and other heavy metals by accumulating the metals in the cell mass, thus allowing for better plant growth at mM concentrations of heavy metals [124]. The amount of Ni in Lastensuo did not appear to have any effect on bacterial numbers, indicating that the concentrations found were not high enough to be toxic to the microorganisms (Figure 7). Commercially available peat has successfully been used as sorbent for the removal of Ni from aqueous solutions [125], indicating that the peat itself may sorb the Ni and perhaps that is why there is a specific layer where the Ni appears to be enriched

in the peat profile. Nevertheless, bacterial strains originating from Lastensuo have been shown to accumulate Ni intracellularly as well as by sorption to cell surfaces [23].

Silver appeared to be much more influenced by the number of bacteria in the samples, compared to Ni (Figure 7). Although the number of bacteria did not correlate positively or negatively with the concentration of Ag, nor did any microbial taxa, the highest Ag sorption values coincided with the highest bacterial numbers. Only *Lokiarchaea* and *Methanosaeta* correlated negatively with Ag^+ sorption data, and they were present only in the lowest gyttja and clay layers, where Ag^+ sorption was on average only 65% of the sorption observed in the upper peat layers. Ag was present in all bog layers evenly distributed in low concentration (0.01–0.02 mg/kg DW), which was possibly too low to have toxic effects on the microbial communities [126]. The Ag^+ ion is a known bactericide but reports about its efficiency against archaea is scarce. Silver nanoparticles have however shown potent antimicrobial activity against, e.g., *Haloarchaea* [80] at the concentrations exceeding the extracted Ag concentrations observed in our study (300–400 $\mu\text{g}/\text{mL}$ vs. ~ 0.01 – 0.02 $\mu\text{g}/\text{mL}$). Nevertheless, bacterial strains isolated from the Lastensuo Bog have been shown to remove Ag from solution by yet unknown mechanisms [127]. The same study estimated that less than 0.2% of the Ag sorption in the peat, gyttja, and clay layers is due to bacteria, whereas in the surface moss, this proportion was 2.3%

In addition to positive correlations between Cs concentration and archaeal and bacterial taxa, specific parts of the archaeal and bacterial communities also correlated positively and significantly with Cs (Cs^+) batch sorption data. However, the microorganisms correlating with Cs sorption were almost exclusively detected in the gyttja and clay layers (Figures A3 and A4), where also the highest Cs^+ retention (K_d value) and Cs concentrations were recorded. However, the bacterial numbers in the different bog layers did not correlate with the concentration or retention of Cs. The accumulation of Cs on the lowest clay layer is expected, as clays have high cation exchange capacity and the pH of the layer is higher. This is because the surface charge is dependent on the pH and cation sorption typically decreases as the pH decreases. Previously, we observed the deepest clay layer behaving somewhat differently from the upper layers as the effect of pH change on Cs sorption was less prominent than in the upper organic layers [38]. However, in the upper organic layers, the sorption K_d values reached those of the lowest clay layer, but not until alkaline pH was recorded [38]. In the clay layer, Cs retention maximum was found at pH 8.9 as in the upper layers the corresponding maximum was between pH 6.7 and 9.6 depending on the layer [38]. Peat typically has a broad spectrum of pKa values, due to various protonating groups like carboxylic groups, alcoholic, and phenolic OH groups as well as amino groups (see, e.g., in [128–131]). For clay minerals, like illite present in the lowest layer, pKa values from 4.2 to 9.0 have been reported (see, e.g., in [132]). On mineral surfaces sorption takes place via two separate mechanisms namely outer-sphere and inner-sphere complexation on which sorption occurs on hydroxyl groups or through sorption on interlayers and frayed edge sites (FES sites) of clay minerals [133]. Sorption takes place between charged surfaces and partially or fully hydrated ions. Clay minerals are characterized by permanent negative charge [35], which is stabilized by exchangeable cations adsorbed on the basal planes or interlayer spaces of these minerals. In the case of partly or fully dehydrated Cs^+ ions, inner-sphere complexes are formed directly to the siloxane groups of clay minerals (especially illite) within the interlayer or at the FES site [35,133]. Microorganisms are not expected to affect the formation of these inner-sphere complexes, and typically the higher clay content increases the straight sorption of various metals on clay mineral ion-exchange sites. Therefore, it seems most probable, that the change in the pH and mineral content controls the sorption of Cs in this layer and at the same time the change in the microbial community is seen because of the changes in the layer chemical, physical and mineralogical properties, resulting in positive correlation between bacterial and archaeal taxa and Cs concentrations.

Previously, microbiota have been shown to affect the retention of SeO_3^{2-} in this acidic nutrient-poor bog environment under oxic conditions and the retention mechanisms most

likely include the formation of reduced Se^0 [58,64]. In present study, strong correlation between bacterial numbers and selenium retention both under oxic and anoxic conditions was seen. The mechanism here is not known, but under aerobic or microaerophilic conditions, SeO_3^{2-} can be reduced by several bacterial strains using detoxification or redox homeostasis, possible reactions including, e.g., Painter-type reactions, thioredoxin reductase system, and sulfide-mediated reduction [62] facilitating Se retention. In the present study, the speciation of selenium was not determined, but, e.g., *Pseudomonas* spp. And *Burkholderia* spp. Strains isolated from Lastensuo peat grown with SeO_3^{2-} under oxic conditions effectively remove SeO_3^{2-} from the nutrient solutions, presumably by a detoxification reaction and *Pseudomonas* sp. Has been shown to accumulate reduced Se^0 inside the cell [58,64,134]. However, these bacteria were present at only very low relative abundances of <3%, and no correlation with SeO_3^{2-} retention under aerobic conditions and these bacterial groups was observed. In addition, under anoxic conditions the number of bacteria correlated with the retention of Se (Table 7, Figure 7). Under anoxic (reducing) conditions, slow abiotic reduction (>1month) in the presence of Fe(II) is possible [66], and in addition several bacteria may use SeO_3^{2-} or SeO_4^{2-} as terminal electron acceptors also under anoxic conditions and reduce soluble $\text{SeO}_3^{2-}/\text{SeO}_4^{2-}$ to Se^0 (see, e.g., in [134,135]). This occurs predominantly via microbial dissimilatory reduction with organic substrates, such as acetate, lactate and ethanol, or hydrogen as electron donors [61]. Dissimilatory Se reduction to Se^0 one of the most important sinks for Se oxyanions under anoxic environments [136] and SeO_4^{2-} reductases have been identified in the genomes of, e.g., *Anaerolineaceae* [137], which in present study were present mainly in the lowest gyttja layer, with 2% abundance. However, correlation between these bacteria and selenium retention was not seen in present study. Microbial reduction of oxyanionic selenium species (SeO_3^{2-} and SeO_4^{2-}) into insoluble elemental Se^0 is important especially in the organic wetland environments affecting selenium mobility [138]. However, in addition to the microbial-mediated processes, in suboxic and anoxic Fe(II,III) oxide- and sulfide (S^{2-})-containing environments, gradual abiotic reduction of SeO_3^{2-} to Se^0 is also important [66,139].

No statistically significant correlation between microbial groups or bacterial numbers and sorption of I in aerobic conditions was identified. However, the regression analysis showed slightly higher I sorption with higher bacterial numbers and low sorption in the clay layer (Figure 7C,D), indicating that bacterial biomass may somewhat affect the I retention in aerobic conditions. In soil organic matter, iodine sorption has been suggested to occur through catalytic oxidation of I^- into reactive iodine species, such as I_2 and HIO , by environmental (microbial) peroxides, which after reactive iodine is bound into organic matter (forming org-I), see, e.g., in [77]. Peatlands are considered the most important sinks of terrestrial iodine and peatland micro- and macroalgae, fungi, and bacteria facilitate the iodine redox cycle by I^- oxidation and formation of org-I, but also by dehalogenation of org-I, and reduction of oxidized iodine species to I^- [140], e.g., *Anaerolineae* (a genus of *Anaerolineaceae*) has been previously shown to reductively deiodinize benzene derivatives [140]. However, in present study, we observed a strong positive correlation (Table 7) between *Anaerolineaceae* and anaerobic iodine retention. These bacteria were present mainly in the gyttja layer, where interactions between organic matter and increasing proportion of clay may occur, resulting in complex iodine geochemistry as well as changes in the microbial populations. The lack of correlation between bacterial numbers and iodine sorption data may result from the more important role of fungi in the iodine cycle, which has also been suggested in previous studies, see, e.g., in [140].

Cu is known to be toxic for bacteria and fungi and the toxicity increases with decreasing pH [141]. In our study, only *Lokiarchaeia* and the MSBL5 of the *Chloroflexi* showed any effects to Cu and both correlated positively with the highest concentration of Cu in the clay layer. However, the concentration of Cu in Lastensuo was low or similar compared to boreal peatlands and podzols and agricultural soils [2,142]. However, Cu concentrations may increase in the vicinity of SNF repositories if Cu is leached from exposed waste canisters. Zn is another putatively toxic metal for microorganisms. Zn may reduce the

microbial diversity in agricultural soils at levels of 400 mg kg^{-1} [143]. One study showed that culturable soil bacteria may be susceptible to zinc at concentrations of 2.5 mM (approximately 180 mg L^{-1}) in their growth medium [144]. However, this is still a significantly higher concentrations than what we found in the bog samples, which are in line with Zn concentrations found in other boreal peatlands [2]. In Lastensuo, only Hadarchaeales and uncultured Methanomicrobiaceae correlated with the concentration of Zn, but these archaea were mostly found in the clay layer, where the Zn concentration also was the highest, indicating that the clay layer itself may be a stronger driver for these archaea than the concentration of Zn.

Our present study supports our previous assumptions [38,64] that microbial populations can contribute partly to Se and I retention in this ombrotrophic boreal environment. The role of microbial populations in the retention behavior of Cs, Ag, and Ni appears to be less pronounced although certain archaea may affect to Ag environmental behavior.

Finally, fungi did not correlate strongly with any physicochemical parameter or with sorption data, although fungi were detected throughout the bog profile. Our work is one of the few that has investigated the relative abundances of fungi present throughout the depth profile of an oligotrophic boreal bog. Nevertheless, the importance of fungi as decomposers increases in nutrient-poor conditions [145]. *Phaeoacremonium* was the most prominent fungal genus in all other samples but the surface moss with an increasing relative abundance in the deeper peat layers (Figure A2). This fungus has been shown to produce high amounts of manganese peroxidases in anoxic lake sediment, thus promoting anoxic degradation of lignin [146]. Although anaerobic degradation of recalcitrant carbon compounds in deep peat environments has been shown to be low [147], anaerobic degradation of recalcitrant organic matter to more easily utilized sugars by fungi could support a diverse prokaryotic community in oligotrophic and anaerobic bogs [148].

5. Conclusions

The Lastensuo Bog area has high bacterial, archaeal, and fungal diversity, and especially several bacterial and archaeal groups seemed adapted to the variable concentrations of heavy metals, alkali metals, as well as radionuclides from natural decay chains of uranium (U and Th). The present data indicate that the archaeal and bacterial communities in the deep bog layers (namely gyttja and clay) tolerate high concentrations of metals and may concurrently contribute to the total retention of metals and radionuclides in these layers. At the same time, it is probable that a change in chemical, mineralogical, and physical factors (pH, redox potential, and mineral content) present in this ombrotrophic boreal environment is affecting both the microbial population and the retention of metals. However, more research on the toxicity of the metals on various parts of the microbial community present in this area is still needed.

Author Contributions: Conceptualization, M.L. and M.B.; methodology, M.L. and M.B.; software, M.L. and M.B.; formal analysis, M.L. and M.B.; investigation, M.L.; writing—original draft preparation, M.L.; writing—review and editing, M.L. and M.B. All authors have read and agreed to the published version of the manuscript.

Funding: This research received no external funding.

Institutional Review Board Statement: Not applicable.

Informed Consent Statement: Not applicable.

Data Availability Statement: The data sequence data sets presented in this study are available from European Nucleotide Archive (ENA, <http://www.ebi.ac.uk/ena>) under Study accession numbers PRJEB6875 (bacteria) and PRJEB41440 (archaea, fungi). All other used data is presented in the tables and references of the paper.

Conflicts of Interest: The authors declare no conflict of interest.

Appendix A

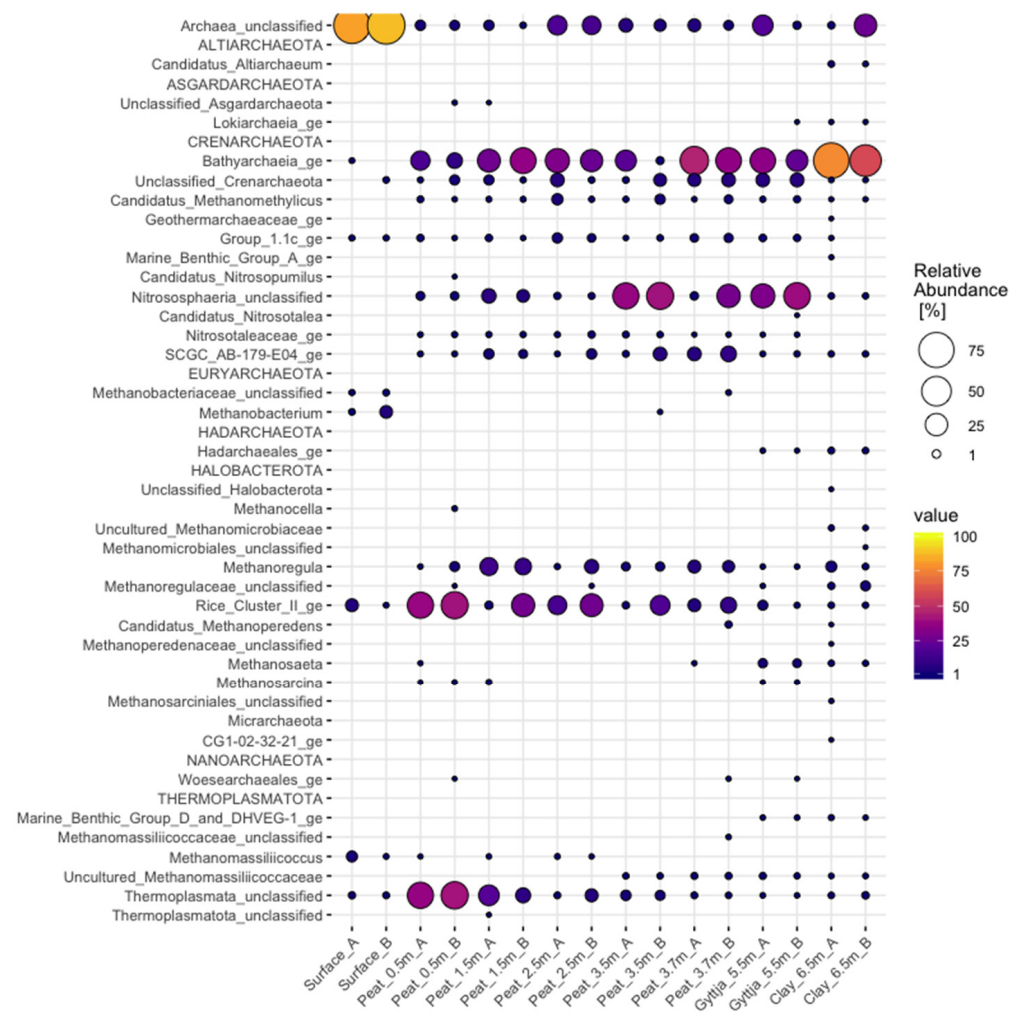


Figure A1. Relative abundance of archaeal genera in surface moss, peat, gyttja, and clay samples collected from Lastensuo bog.

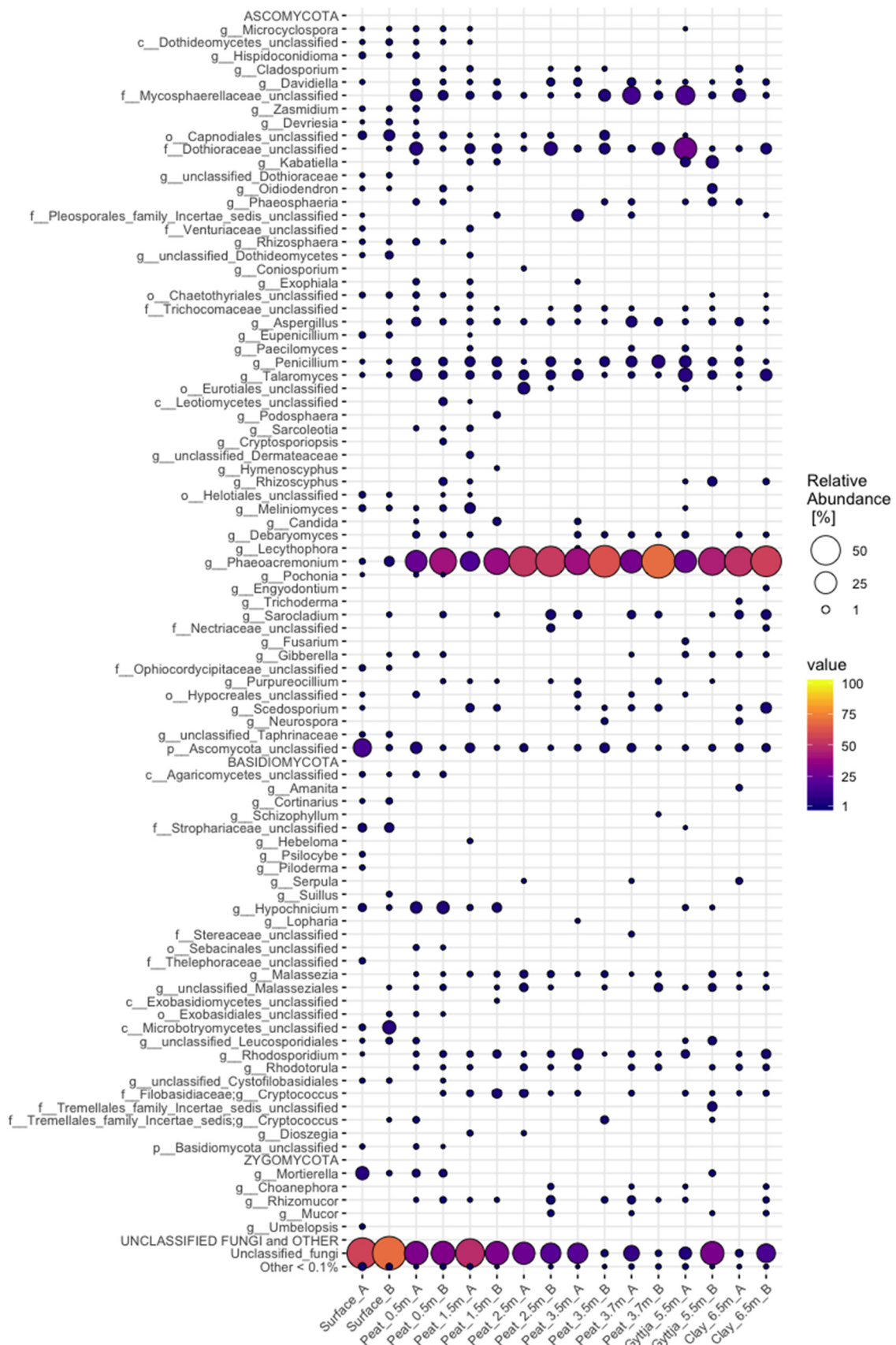


Figure A2. Relative abundance of fungal genera in surface moss, peat, gyttja, and clay samples collected from Lastensuo bog.

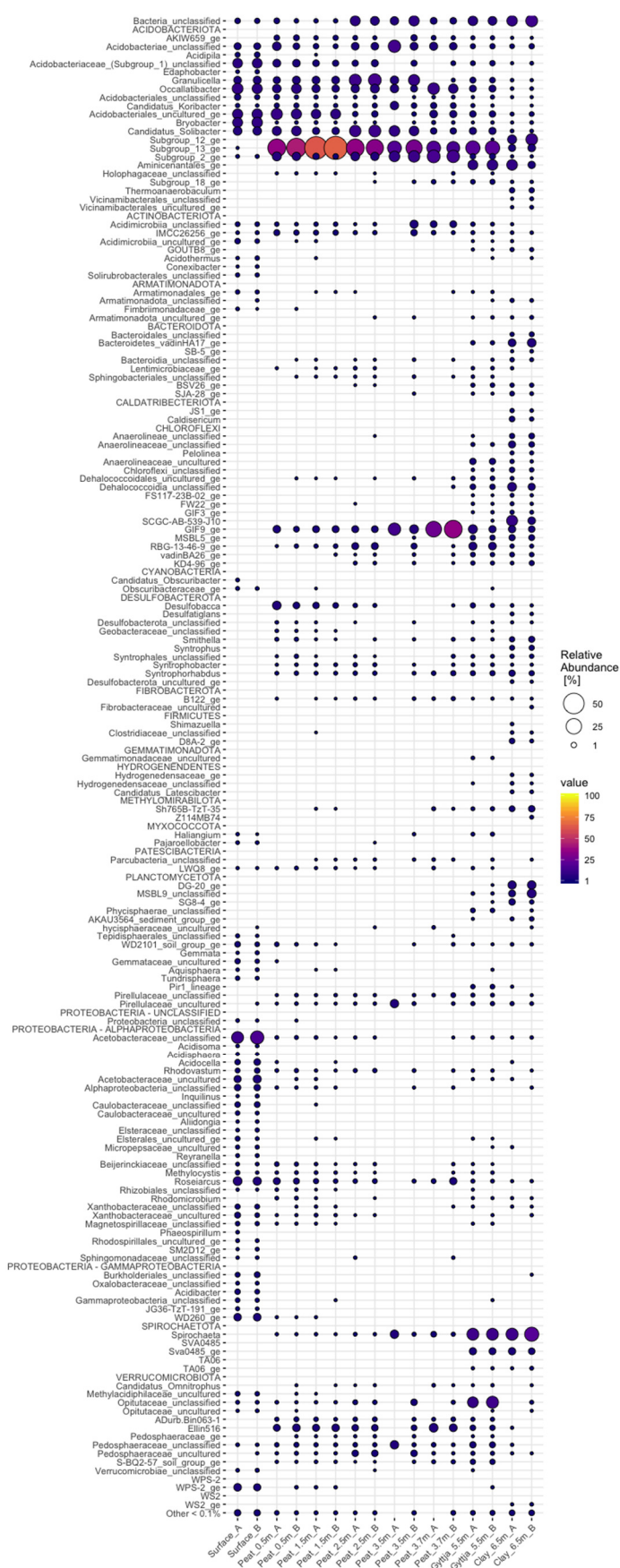


Figure A3. The relative abundance of the bacterial genera (% of sequence reads) in the Lastensuo bog samples.

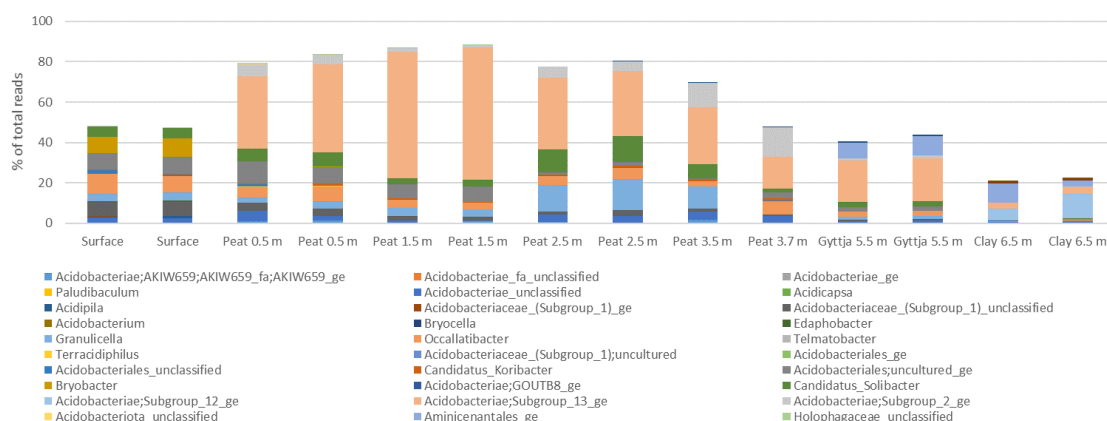


Figure A4. The relative abundance of Acidobacteriota genera in Lastensuo Bog samples.

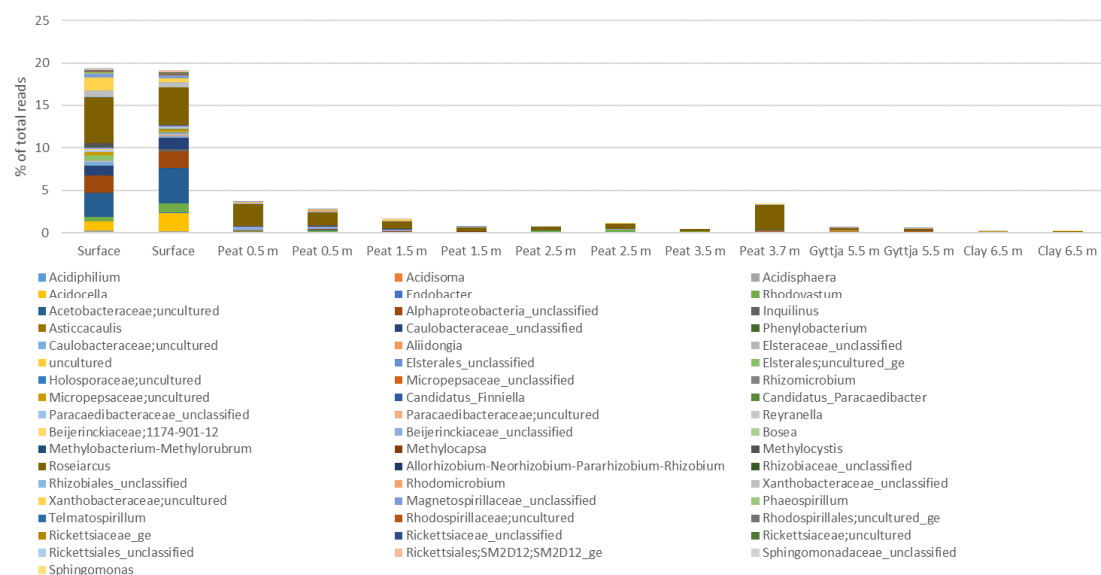


Figure A5. The relative abundance of Alphaproteobacterial genera in Lastensuo Bog samples.

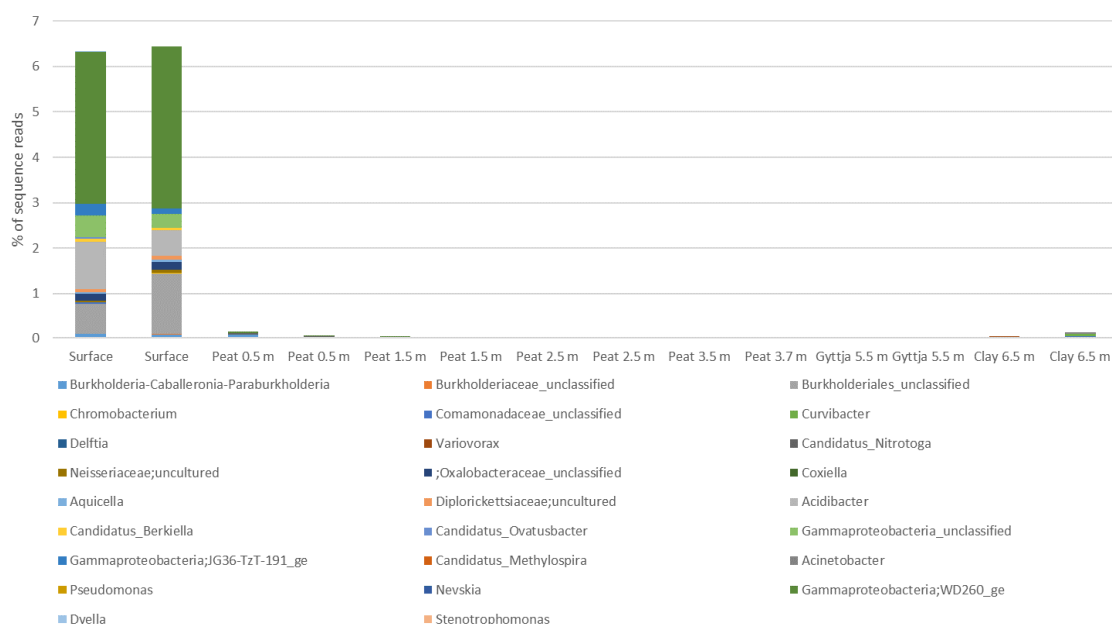


Figure A6. The relative abundance of Gammaproteobacterial genera in Lastensuo Bog samples.

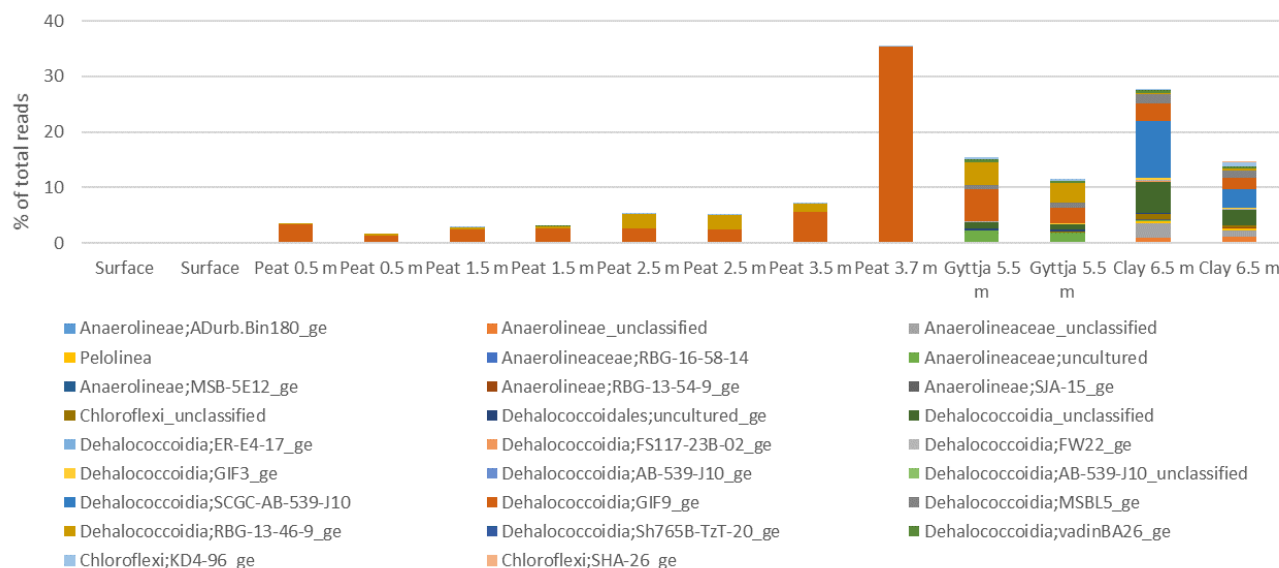


Figure A7. The relative abundance of Chloroflexi genera in Lastensuo Bog samples.

Table A1. Pearson correlation coefficients of the Bonferroni corrected correlations between relative abundance of archaeal genera and physicochemical parameters and metal concentrations. Correlation coefficients for pairs with $p < 0.05$ are shown.

	Candidatus Altiarchaeum	Lokiarchaeia Genus	Crenarchaeota Unclassified	HADARCHAEALES GENUS	Methanomicrobiaceae Uncultured	Methanosaeta	Methanomassiliicoccaceae Uncultured
pH		0.98 ***		0.92 **	0.85	0.98 ***	0.86
Eh		−0.98					
Humification degree			0.88				
Organic matter				−0.98 ***	−0.96 ***	−0.92 **	−0.90
Mg		0.88		0.91 *	0.89*	0.85	0.93 **
Fe	0.88	0.94 **		0.98 ***	0.96 ***	0.92 *	0.90 *
Co	0.88	0.96 **		0.99 ***	0.96 ***	0.93 **	0.90 *
Cu		0.90 *				0.91 *	
Zn				0.88	0.88		
Se	0.88	0.93 **		0.98 ***	0.96 ***	0.90 *	0.89 *
Cs	0.88	0.93 **		0.98 ***	0.96 ***	0.90 *	0.89 *
Th	0.87	0.97 ***		0.99 ***	0.95 ***	0.95 ***	0.90 *
U	0.86	0.98 ***		0.98 ***	0.93 **	0.97 ***	0.90 *

* $p < 0.001$, ** $p < 0.0001$, *** $p < 0.00001$.

Table A2. Pearson correlation coefficients of the Bonferroni-corrected correlations between relative abundance of bacterial genera and physicochemical parameters and metal concentrations. Correlation coefficients for pairs with $p < 0.05$ are shown.

	pH	Organic Matter	Mg	Al	Fe	Co	Cu	Se	Cs	Th	U
Acetothermii	0.95	−1.0 ***	0.92		1.0 ***	0.99 ***		1.0 ***	1.0 ***	0.99 ***	0.97 ***
GOUTB8		−1.0 ***	0.92		1.0 ***	1.0 ***		0.99 ***	0.99 ***	1.0 ***	0.98 ***
Acidobacteriae					0.94	0.93		0.94	0.94	0.93	
Subgroup 12											
Thermoanaerobaculum		−1.0 ***	0.92		1.0 ***	0.99 ***		1.0 ***	1.0 ***	0.99 ***	0.97 ***
Vicinamibacteriales					0.92	0.92		0.93	0.92	0.92	
uncultured											
Bacteroidales					0.94	0.93		0.94	0.94	0.93	
unclassified											
Bacteroidetes					0.98 ***	0.98 ***		0.98 ***	0.98 ***	0.98 ***	0.97 ***
vadinHA17		−0.98 ***									
Prolixibacteraceae		−0.98 ***			0.98 ***	0.98 ***		0.98 ***	0.98 ***	0.97 ***	0.95 ***
BSV13											
BSV26				0.92							
Anaerolineae		−0.98 ***			0.98 ***	0.98 ***		0.98 ***	0.98 ***	0.97 ***	0.95 *
unclassified											
Pelolinea		−1.0 ***	0.93		1.0 ***	1.0 ***		1.0 ***	1.0 ***	0.99 ***	0.97 ***
SJA-15		−0.96			0.96 *	0.95 *		0.98 *	0.96 *	0.95	0.93
Chloroflexi					0.91	0.92				0.91	
unclassified											
Dehalococcoidia					0.92	0.93				0.94	0.94
unclassified											
GIF3	0.98 ***				0.94	0.94		0.93	0.93	0.95	0.95 *
MSBL5							0.94			0.92	0.96 *
vadinBA26				0.94							
Desulfatiglan					0.93	0.92		0.93	0.93	0.92	
Smithella					0.93	0.92		0.93	0.93	0.92	
Syntrophus		−0.99 ***	0.92		1.0 ***	0.99 ***		0.99 ***	0.99 ***	0.98 ***	0.96 *
Firmicutes		−0.96			0.96 *	0.95 *		0.96 *	0.96 *	0.96	0.93
unclassified											
TSAC18		−0.96			0.96 *	0.95 *		0.96 *	0.96 *	0.95	0.93
Hydrogenedensaceae		−0.99 ***	0.91		0.99 ***	0.98 ***		0.99 ***	0.99 ***	0.98 ***	0.96 *
Candidatus		−0.98 **			0.98 ***	0.98 ***		0.98 ***	0.98 ***	0.97 ***	0.95
Latescibacter											
Latescibacteraceae	0.94	−1.0 ***	0.92		1.0 ***	0.99 ***		1.0 ***	1.0 ***	0.99 ***	0.97 ***
unclassified											
Methylomirabilaceae		−0.97 *	0.92		0.97 ***	0.97 ***		0.96 ***	0.96 *	0.97 ***	0.97 ***
Sh765B-TzT-35											
MidBa8		−1.0 ***	0.92		1.0 ***	0.99 ***		1.0 ***	1.0 ***	0.99 ***	0.97 ***
DG-20		−1.0 ***	0.92		1.0 ***	0.99 ***		1.0 ***	1.0 ***	0.99 ***	0.97 ***
MSBL9					0.93	0.92		0.93	0.93	0.92	
unclassified											
AKAU3564		−0.96			0.95 *	0.95 *		0.95 *	0.95 *	0.95	0.93
sediment group											
Planctomycetota		−0.94									
unclassified											
Spirochaeta				0.93							
Sva0485				0.93							
WCHB1-41		−0.96			0.96 *	0.95 *		0.96 *	0.96 *	0.95	0.93

* $p < 0.001$, ** $p < 0.0001$, *** $p < 0.00001$.

References

- Hovmand, M.F.; Kemp, K.; Kystol, J.; Johnsen, I.; Riis-Nielsen, T.; Pacyna, J.M. Atmospheric heavy metal deposition accumulated in rural forest soils of southern Scandinavia. *Environ. Pollut.* **2008**, *155*, 537–541. [\[CrossRef\]](#) [\[PubMed\]](#)
- Ukonmaanaho, L.; Nieminen, T.M.; Rausch, N.; Shotyk, W. Heavy metal and arsenic profiles in ombrogenous peat cores from four differently loaded areas in Finland. *Water Air Soil Pollut.* **2004**, *158*, 277–294. [\[CrossRef\]](#)
- Laird, K.R.; Das, B.; Cumming, B.F. Enrichment of uranium, arsenic, molybdenum, and selenium in sediment cores from boreal lakes adjacent to northern Saskatchewan uranium mines. *Lake Reserv. Manag.* **2014**, *30*, 344–357. [\[CrossRef\]](#)
- Roberts, S.; Kirk, J.L.; Wiklund, J.A.; Muir, D.C.; Keating, J.; Yang, F.; Gleason, A.; Lawson, G.; Wang, X.; Evans, M. Sources of atmospheric metal (loid) pollution recorded in Thompson Manitoba lake sediment cores within the Canadian boreal biome. *Sci. Total Environ.* **2020**, *732*, 139043. [\[CrossRef\]](#) [\[PubMed\]](#)
- Tchounwou, P.B.; Yedjou, C.G.; Patlolla, A.K.; Sutton, D.J. Heavy metal toxicity and the environment. *Mol. Clin. Environ. Toxicol.* **2012**, *101*, 133–164.
- Sigee, D.C.; Al-Rabae, R.H. Nickel toxicity in *Pseudomonas tabaci*: Single cell and bulk sample analysis of bacteria cultured at high cation levels. *Protoplasma* **1986**, *130*, 171–185. [\[CrossRef\]](#)

7. Rajapaksha, R.M.C.P.; Tobor-Kaplon, M.A.; Bååth, E. Metal toxicity affects fungal and bacterial activities in soil differently. *Appl. Environ. Microbiol.* **2004**, *70*, 2966–2973. [\[CrossRef\]](#)
8. Pennanen, T.; Frostegard, A.S.A.; Fritze, H.; Baath, E. Phospholipid fatty acid composition and heavy metal tolerance of soil microbial communities along two heavy metal-polluted gradients in coniferous forests. *Appl. Environ. Microbiol.* **1996**, *62*, 420–428. [\[CrossRef\]](#)
9. Haapanen, R.; Aro, L.; Lahdenperae, A.M.; Helin, J.; Ikonen, A.T.K. *Studies on Reference Mires: 1. Lastensuo and Pesaensuo in 2010–2011*; No. POSIVA-WR-12-102; Posiva Oy: Eurajoki, Finland, 2013.
10. Hjerpe, T.; Broed, R.; Ikonen, A.T.K. *Biosphere Assessment Report 2009*; No. POSIVA-10-03; Posiva Oy: Eurajoki, Finland, 2010.
11. Dönmez, G.Ç.; Aksu, Z.; Öztürk, A.; Kutsal, T. A comparative study on heavy metal biosorption characteristics of some algae. *Process Biochem.* **1999**, *34*, 885–892. [\[CrossRef\]](#)
12. Wong, J.P.K.; Wong, Y.S.; Tam, N.F.Y. Nickel biosorption by two chlorella species, *C. Vulgaris* (a commercial species) and *C. Miniata* (a local isolate). *Bioresour. Technol.* **2000**, *73*, 133–137. [\[CrossRef\]](#)
13. Aksu Ksu, Z. Determination of the equilibrium, kinetic and thermodynamic parameters of the batch biosorption of nickel (II) ions onto *Chlorella vulgaris*. *Process Biochem.* **2002**, *38*, 89–99. [\[CrossRef\]](#)
14. Grandjean, P. *Human Exposure to Nickel*; IARC Scientific Publications: Lyon, France, 1984; pp. 469–485.
15. Scott-Fordsmand, J.J. Toxicity of nickel to soil organisms in Denmark. *Rev. Environ. Contam. Toxicol.* **1997**, *148*, 1–34.
16. Gupta, V.K.; Rastogi, A.; Nayak, A. Biosorption of nickel onto treated alga (*Oedogonium hatei*): Application of isotherm and kinetic models. *J. Colloid Interface Sci.* **2010**, *342*, 533–539. [\[CrossRef\]](#) [\[PubMed\]](#)
17. Akhtar, N.; Iqbal, J.; Iqbal, M. Removal and recovery of nickel (II) from aqueous solution by loofa sponge-immobilized biomass of *Chlorella sorokiniana*: Characterization studies. *J. Hazard. Mater.* **2004**, *108*, 85–94. [\[CrossRef\]](#) [\[PubMed\]](#)
18. White, C.E.; Wilkinson, S.C.; Gadd, G.M. The role of microorganisms in biosorption of toxic metals and radionuclides. *Intern. Biodeterior. Biodegrad.* **1995**, *35*, 17–40. [\[CrossRef\]](#)
19. Ledin, M.; Pedersen, K. The environmental impact of mine wastes—Roles of microorganisms and their significance in treatment of mine wastes. *Earth-Sci. Rev.* **1996**, *41*, 67–108. [\[CrossRef\]](#)
20. López, A.; Lázaro, N.; Priego, J.M.; Marqués, A.M. Effect of pH on the biosorption of nickel and other heavy metals by *Pseudomonas fluorescens* 4F39. *J. Ind. Microbiol. Biotechnol.* **2000**, *24*, 146–151. [\[CrossRef\]](#)
21. Sar, P.; Kazy, S.K.; Singh, S.P. Intracellular nickel accumulation by *Pseudomonas aeruginosa* and its chemical nature. *Lett. App. Microbiol.* **2001**, *32*, 257–261. [\[CrossRef\]](#)
22. Mulrooney, S.B.; Hausinger, R.P. Nickel uptake and utilization by microorganisms. *FEMS Microbiol. Rev.* **2003**, *27*, 239–261. [\[CrossRef\]](#)
23. Knuutinen, J.; Bomberg, M.; Kemell, M.; Lusa, M. Ni(II) interactions in boreal *Peaenibacillus* sp., *Methylobacterium* sp., *Paraburkholderia* sp. and *Pseudomonas* sp. strains isolated from an acidic, ombrotrophic bog. *Front. Microbiol.* **2019**. [\[CrossRef\]](#)
24. Eitinger, T.; Mandrand-Berthelot, M.-A. Nickel transport systems in microorganisms. *Arch. Microbiol.* **2000**, *173*, 1–9. [\[CrossRef\]](#) [\[PubMed\]](#)
25. Pedroso, M.S.; Pinho, G.L.; Rodrigues, S.C.; Bianchini, A. Mechanism of acute silver toxicity in the euryhaline copepod *Acartia tonsa*. *Aquat. Toxicol.* **2007**, *82*, 173–180. [\[CrossRef\]](#) [\[PubMed\]](#)
26. Jacobson, A.R.; McBride, M.B.; Baveye, P.; Steenhuis, T.S. Environmental factors determining the trace-level sorption of silver and thallium to soils. *Sci. Total Environ.* **2005**, *345*, 191–205. [\[CrossRef\]](#) [\[PubMed\]](#)
27. Smith, I.; Carson, B. *Silver*; MI7 Ann Arbor Science Publishers: Ann Arbor, MI, USA, 1977.
28. Hadrup, N.; Sharma, A.K.; Loeschner, K. Toxicity of silver ions, metallic silver, and silver nanoparticle materials after in vivo dermal and mucosal surface exposure: A review. *Regul. Toxicol. Pharmacol.* **2018**, *98*, 257–267. [\[CrossRef\]](#)
29. Rosenman, K.D.; Seixas, N.; Jacobs, I. Potential nephrotoxic effects of exposure to silver. *Occup. Environ. Med.* **1987**, *44*, 267–272. [\[CrossRef\]](#)
30. Das, D.; Das, N.; Mathew, L. Kinetics, equilibrium and thermodynamic studies on biosorption of Ag (I) from aqueous solution by macrofungus *Pleurotus platypus*. *J. Hazard. Mater.* **2010**, *184*, 765–774. [\[CrossRef\]](#)
31. SKB. *Long-Term Safety for the Final Repository for Spent Nuclear Fuel at Forsmark Main Report of the SR-Site Project Volume III*; Errata 2011-10, SKB TR-11-01; Svensk Kärnbränslehantering AB: Stockholm, Sweden, 2011.
32. Williams, M.; Wohlers, D.W.; Citra, M.; Diamond, G.L.; Swarts, S.G. *Toxicological profile of Cesium*; U.S. Department of Health and Human Services, Public Health Service Agency for Toxic Substances and Disease Registry: Atlanta, GA, USA, 2004.
33. Sparks, D.L. *Environmental Soil Chemistry*; Elsevier: Amsterdam, The Netherlands, 2003.
34. Helin, J.; Ikonen, A.T.K.; Hjerpe, T. *Review of Element-Specific Data for Biosphere Assessment BSA-2009*; Working Report 2010-37; Posiva Oy: Eurajoki, Finland, 2010.
35. Bostick, B.C.; Vairavamurthy, M.A.; Karthikeyan, K.G.; Chorover, J. Cesium adsorption on clay minerals: An EXAFS spectroscopic investigation. *Environ. Sci. Technol.* **2002**, *36*, 2670–2676. [\[CrossRef\]](#)
36. Chang, K.P.; Hsu, C.N.; Tamaki, H. Basic study of ¹³⁷Cs sorption on soil. *J. Nucl. Sci. Technol.* **1993**, *30*, 1243–1247. [\[CrossRef\]](#)
37. Zhuang, J.; Flury, M.; Jin, Y. Colloid-facilitated Cs transport through water-saturated Hanford sediment and Ottawa sand. *Environ. Sci. Technol.* **2003**, *37*, 4905–4911. [\[CrossRef\]](#)
38. Lusa, M.; Bomberg, M.; Virtanen, S.; Lempinen, J.; Aromaa, H.; Knuutinen, J.; Lehto, J. Factors affecting the sorption of cesium in a nutrient-poor boreal bog. *J. Environ. Radioact.* **2015**, *147*, 22–32. [\[CrossRef\]](#)

39. Sasaki, T.; Kubota, T.; Mito, S.; Kauri, T.; Kudo, A. Radionuclide sorption to a mixture of anaerobic bacteria in the repository environment. *J. Nucl. Sci. Technol.* **2002**, *39* (Suppl. 3), 954–957. [\[CrossRef\]](#)
40. Higo, M.; Kang, D.J.; Isobe, K. First report of community dynamics of arbuscular mycorrhizal fungi in radiocesium degradation lands after the Fukushima-Daiichi Nuclear disaster in Japan. *Sci. Rep.* **2019**, *9*, 1–10. [\[CrossRef\]](#) [\[PubMed\]](#)
41. Ohnuki, T.; Sakamoto, F.; Kozai, N.; Nanba, K.; Neda, H.; Sasaki, Y.; Niizato, T.; Watanabe, N.; Kozaki, T. Role of filamentous fungi in migration of radioactive cesium in the Fukushima forest soil environment. *Environ. Sci. Process. Impacts* **2019**, *21*, 1164–1173. [\[CrossRef\]](#) [\[PubMed\]](#)
42. Gyuricza, V.; Thiry, Y.; Wannijn, J.; Declerck, S.; Dupré de Boulois, H. Radiocesium transfer between *Medicago truncatula* plants via a common mycorrhizal network. *Environ. Microbiol.* **2010**, *12*, 2180–2189. [\[PubMed\]](#)
43. Coppin, F.; Chabrouillet, C.; Martin-Garin, A. Selenite interactions with some particulate organic and mineral fractions isolated from a natural grassland soil. *Eur. J. Soil Sci.* **2009**, *60*, 369–376. [\[CrossRef\]](#)
44. Sharmasarkar, S.; Vance, G.F. Soil and plant selenium at a reclaimed uranium mine. *J. Environ. Qual.* **2002**, *31*, 1516–1521. [\[CrossRef\]](#)
45. Manceau, A.; Gallup, D.L. Removal of Selenocyanate in Water by Precipitation: Characterization of Copper–Selenium Precipitate by X-ray Diffraction, Infrared, and X-ray Absorption Spectroscopy. *Environ. Sci. Technol.* **1997**, *31*, 968–976. [\[CrossRef\]](#)
46. Yasin, M.; El Mehdawi, A.F.; Jahn, C.E.; Anwar, A.; Turner, M.F.; Faisal, M.; Pilon-Smits, E.A. Seleniferous soils as a source for production of selenium-enriched foods and potential of bacteria to enhance plant selenium uptake. *Plant Soil* **2015**, *386*, 385–394. [\[CrossRef\]](#)
47. De Souza, M.P.; Chu, D.; Zhao, M.; Zayed, A.M.; Ruzin, S.E.; Schichnes, D.; Terry, N. Rhizosphere bacteria enhance selenium accumulation and volatilization by Indian mustard. *Plant Physiol.* **1999**, *119*, 565–574. [\[CrossRef\]](#)
48. Barceloux, D.G. Selenium. *J. Toxicol. Clin. Toxicol.* **1999**, *37*, 145–172. [\[CrossRef\]](#)
49. Xu, C.; Zhang, S.; Ho, Y.-F.; Miller, E.J.; Roberts, K.A.; Li, H.-P.; Schwehr, K.A.; Otsuka, S.; Kaplan, D.I.; Brinkmeyer, R.; et al. Is soil natural organic matter a sink or source for mobile radioiodine (¹²⁹I) at the Savannah River Site? *Geochim. Cosmochim. Acta* **2011**, *75*, 5716–5735. [\[CrossRef\]](#)
50. World Health Organization. *Trace Elements in Human Nutrition and Health*; World Health Organization: Geneva, Switzerland, 1996.
51. Antonyak, H.; Iskra, R.; Panas, N.; Lysiuk, R. Selenium. In *Trace Elements and Minerals in Health and Longevity*; Springer International Publishing: Berlin/Heidelberg, Germany, 2018.
52. Oldfield, J.E. *Selenium World Atlas*; Selenium-Tellurium Development Association (STDA): Grimbergen, Belgium, 2002.
53. Fleming, G.A.; Walsh, T. Selenium occurrence in certain Irish soils and its toxic effects on animals. In *Proceedings of the Royal Irish Academy. Section B: Biological, Geological, and Chemical Science*; Hodges, Figgis, Co.: Dublin, Ireland, 1956; pp. 151–166.
54. Li, H.F.; McGrath, S.P.; Zhao, F.J. Selenium uptake, translocation and speciation in wheat supplied with selenate or selenite. *New Phytol.* **2008**, *178*, 92–102. [\[CrossRef\]](#)
55. Bebie, M.; Chauvin, J.P.; Adriano, J.M.; Grosse, S.; Verméglio, A. Effect of selenite on growth and protein synthesis in the phototrophic bacterium *Rhodobacter sphaeroides*. *Appl. Environ. Microbiol.* **2001**, *67*, 4440–4447. [\[CrossRef\]](#)
56. Tarze, A.; Dauplais, M.; Grigoros, I.; Lazard, M.; Ha-Duong, N.-T.; Barbier, F.; Blanquet, S.; Plateau, P. Extracellular production of hydrogen selenide accounts for thiol-assisted toxicity of selenite against *Saccharomyces cerevisiae*. *J. Biol. Chem.* **2007**, *282*, 8759–8767. [\[CrossRef\]](#)
57. Oremland, R.S.; Herbel, M.J.; Blum, J.S.; Langley, S.; Beveridge, T.J.; Ajayan, P.M.; Sutto, T.; Ellis, A.V.; Curran, S. Structural and spectral features of selenium nanospheres produced by Se-respiring bacteria. *Appl. Environ. Microbiol.* **2004**, *70*, 52–60. [\[CrossRef\]](#)
58. Lusa, M.; Knuutinen, J.; Bomberg, M. Uptake and reduction of Se (IV) in two heterotrophic aerobic *Pseudomonas* strains isolated from boreal bog environment. *AIMS Microbiol.* **2017**, *3*, 798. [\[CrossRef\]](#)
59. Oremland, R.S.; Steinberg, N.A.; Maest, A.S.; Miller, L.G.; Hollibaugh, J.T. Measurement of in situ rates of selenate removal by dissimilatory bacterial reduction in sediments. *Environ. Sci. Technol.* **1990**, *24*, 1157–1164. [\[CrossRef\]](#)
60. Zhang, Y.; Moore, J.N. Selenium fractionation and speciation in a wetland system. *Environ. Sci. Technol.* **1996**, *30*, 2613–2619. [\[CrossRef\]](#)
61. Stolz, J.F.; Oremland, R.S. Bacterial respiration of arsenic and selenium. *FEMS Microbiol. Rev.* **1999**, *23*, 615–627. [\[CrossRef\]](#)
62. Nanchaiah, Y.V.; Lens, P.N.L. Ecology and biotechnology of selenium-respiring bacteria. *Microbiol. Mol. Biol. Rev.* **2015**, *79*, 61–80. [\[CrossRef\]](#) [\[PubMed\]](#)
63. De Souza, M.P.; Huang, C.P.A.; Chee, N.; Terry, N. Rhizosphere bacteria enhance the accumulation of selenium and mercury in wetland plants. *Planta* **1999**, *209*, 259–263. [\[CrossRef\]](#)
64. Lusa, M.; Help, H.; Honkanen, A.P.; Knuutinen, J.; Parkkonen, J.; Kalasová, D.; Bomberg, M. The reduction of selenium (IV) by boreal *Pseudomonas* sp. strain T5-6-I—Effects on selenium (IV) uptake in *Brassica oleracea*. *Environ. Res.* **2019**, *177*, 108642. [\[CrossRef\]](#)
65. Rosenfeld, C.E.; Kenyon, J.A.; James, B.R.; Santelli, C.M. Selenium (IV, VI) reduction and tolerance by fungi in an oxic environment. *Geobiology* **2017**, *15*, 441–452. [\[CrossRef\]](#) [\[PubMed\]](#)
66. Charlet, L.; Scheinost, A.; Tournassat, C.; Greneche, J.-M.; Gehin, A.; Fernández-Martínez, A.; Coudert, S.; Tisserand, D.; Brendle, J. Electron transfer at the mineral/water interface: Selenium reduction by ferrous iron sorbed on clay. *Geochim. Cosmochim. Acta* **2007**, *71*, 5731–5749. [\[CrossRef\]](#)

67. Assemi, S.; Erten, H. Sorption of radioiodine on organic rich soil, clay minerals and alumina. *J. Radioanal. Nucl. Chem.* **1994**, *178*, 193–204. [\[CrossRef\]](#)
68. Evans, G.J.; Hammad, K.A. Radioanalytical studies of iodine behaviour in the environment. *J. Radioanal. Nucl. Chem.* **1995**, *192*, 239–247. [\[CrossRef\]](#)
69. Sheppard, M.I.; Hawkins, J.L. Iodine and microbial interactions in an organic soil. *J. Environ. Radioact.* **1995**, *29*, 91–109. [\[CrossRef\]](#)
70. Ashworth, D.J.; Shaw, G.; Butler, A.P.; Ciciani, L. Soil transport and plant uptake of radio-iodine from near-surface groundwater. *J. Environ. Radioact.* **2003**, *70*, 99–114. [\[CrossRef\]](#)
71. Ashworth, D.J.; Shaw, G. A comparison of the soil migration and plant uptake of radioactive chlorine and iodine from contaminated groundwater. *J. Environ. Radioact.* **2006**, *89*, 61–80. [\[CrossRef\]](#)
72. Li, H.-P.; Yeager, C.M.; Brinkmeyer, R.; Zhang, S.; Ho, Y.-F.; Xu, C.; Jones, W.L.; Schwehr, K.A.; Otsuka, S.; Roberts, K.A.; et al. Bacterial production of organic acids enhances H₂O₂-dependent iodide oxidation. *Environ. Sci. Technol.* **2012**, *46*, 4837–4844. [\[CrossRef\]](#)
73. Bostock, A.C.; Shaw, G.; Bell, J.N.B. The volatilisation and sorption of ¹²⁹I in coniferous forest, grassland and frozen soils. *J. Environ. Radioact.* **2003**, *70*, 29–42. [\[CrossRef\]](#)
74. Yamaguchi, N.; Nakano, M.; Takamatsu, R.; Tanida, H. Inorganic iodine incorporation into soil organic matter: Evidence from iodine K-edge X-ray absorption near-edge structure. *J. Environ. Radioact.* **2010**, *101*, 451–457. [\[CrossRef\]](#) [\[PubMed\]](#)
75. Xu, C.; Miller, E.J.; Zhang, S.; Li, H.-P.; Ho, Y.-F.; A Schwehr, K.; Kaplan, D.I.; Otsuka, S.; A Roberts, K.; Brinkmeyer, R.; et al. Sequestration and remobilization of radioiodine (¹²⁹I) by soil organic matter and possible consequences of the remedial action at Savannah River Site. *Environ. Sci. Technol.* **2011**, *45*, 9975–9983. [\[CrossRef\]](#) [\[PubMed\]](#)
76. Li, H.-P.; Yeager, C.M.; Brinkmeyer, R.; Jones, W.L.; Zhang, S.J.; Xu, C.; Schwehr, K.A.; Santschi, P.H.; Kaplan, D.I.; Yeager, C.M. Iodide accumulation by aerobic bacteria isolated from subsurface sediments of an I-129 contaminated aquifer at the Savannah River Site, South Carolina. *Appl. Environ. Microbiol.* **2011**, *77*, 2153–2160. [\[CrossRef\]](#)
77. Xu, C.; Chen, H.; Sugiyama, Y.; Zhang, S.; Li, H.-P.; Ho, Y.-F.; Chuang, C.-Y.; Schwehr, K.A.; Kaplan, D.I.; Yeager, C.; et al. Novel molecular-level evidence of iodine binding to natural organic matter from Fourier transform ion cyclotron resonance mass spectrometry. *Sci. Total Environ.* **2013**, *449*, 244–252. [\[CrossRef\]](#)
78. Amachi, S.; Mishima, Y.; Shinoyama, H.; Muramatsu, Y.; Fujii, T. Active transport and accumulation of iodide by newly isolated marine bacteria. *Appl. Environ. Microbiol.* **2005**, *71*, 741–745. [\[CrossRef\]](#) [\[PubMed\]](#)
79. Ban-Nai, T.; Muramatsu, Y.; Amachi, S. Rate of iodine volatilization and accumulation by filamentous fungi through laboratory cultures. *Chemosphere* **2006**, *65*, 2216–2222. [\[CrossRef\]](#)
80. Lusa, M.; Bomberg, M.; Aromaa, H.; Knuutinen, J.; Lehto, J. Sorption of radioiodide in an acidic, nutrient-poor boreal bog: Insights into the microbial impact. *J. Environ. Radioact.* **2015**, *143*, 110–122. [\[CrossRef\]](#)
81. Dupont, C.L.; Grass, G.; Rensing, C. Copper toxicity and the origin of bacterial resistance—New insights and applications. *Metallomics* **2011**, *3*, 1109–1118. [\[CrossRef\]](#)
82. Vincent, M.; Duval, R.E.; Hartemann, P.; Engels-Deutsch, M. Contact killing and antimicrobial properties of copper. *J. Appl. Microbiol.* **2018**, *124*, 1032–1046. [\[CrossRef\]](#)
83. Antsotegi-Uskola, M.; Markina-Iñarrairaegui, A.; Ugalde, U. New insights into copper homeostasis in filamentous fungi. *Int. Microbiol.* **2020**, *23*, 65–73. [\[CrossRef\]](#)
84. Richard, D.; Ravigné, V.; Rieux, A.; Facon, B.; Boyer, C.; Boyer, K.; Grygiel, P.; Javegny, S.; Terville, M.; Canteros, B.I.; et al. Adaptation of genetically monomorphic bacteria: Evolution of copper resistance through multiple horizontal gene transfers of complex and versatile mobile genetic elements. *Mol. Ecol.* **2017**, *26*, 2131–2149. [\[CrossRef\]](#)
85. Nies, D.H. Bacterial transition metal homeostasis. In *Molecular Microbiology of Heavy Metals*; Springer: Berlin/Heidelberg, Germany, 2007; pp. 117–142.
86. Rosen, B.P.; Liu, Z. Transport pathways for arsenic and selenium: A minireview. *Environ. Int.* **2009**, *35*, 512–515. [\[CrossRef\]](#)
87. Turner, R.J.; Weiner, J.H.; Taylor, D.E. Selenium metabolism in Escherichia coli. *Biomaterials* **1998**, *11*, 223–227. [\[CrossRef\]](#) [\[PubMed\]](#)
88. Amachi, S. Microbial contribution to global iodine cycling: Volatilization, accumulation, reduction, oxidation, and sorption of iodine. *Microbes Environ.* **2008**, *23*, 269–276. [\[CrossRef\]](#)
89. Gozlan, R.S. Isolation of iodine-producing bacteria from aquaria. *Antonie Leeuwenhoek* **1968**, *34*, 226. [\[CrossRef\]](#) [\[PubMed\]](#)
90. Amachi, S.; Muramatsu, Y.; Akiyama, Y.; Miyazaki, K.; Yoshiki, S.; Hanada, S.; Kamagata, Y.; Ban-Nai, T.; Shinoyama, H.; Fujii, T. Isolation of iodide-oxidizing bacteria from iodide-rich natural gas brines and seawaters. *Microb. Ecol.* **2005**, *49*, 547–557. [\[CrossRef\]](#) [\[PubMed\]](#)
91. Li, H.-P.; Daniel, B.; Creeley, D.; Grandbois, R.; Zhang, S.; Xu, C.; Ho, Y.-F.; Schwehr, K.A.; Kaplan, D.I.; Santschi, P.H.; et al. Superoxide production by a manganese-oxidizing bacterium facilitates iodide oxidation. *Appl. Environ. Microbiol.* **2014**, *80*, 2693–2699. [\[CrossRef\]](#) [\[PubMed\]](#)
92. Amachi, S.; Kimura, K.; Muramatsu, Y.; Shinoyama, H.; Fujii, T. Hydrogen peroxide-dependent uptake of iodine by marine Flavobacteriaceae bacterium strain C-21. *Appl. Environ. Microbiol.* **2007**, *73*, 7536–7541. [\[CrossRef\]](#) [\[PubMed\]](#)
93. Amachi, S.; Minami, K.; Miyasaka, I.; Fukunaga, S. Ability of anaerobic microorganisms to associate with iodine: ¹²⁵I tracer experiments using laboratory strains and enriched microbial communities from subsurface formation water. *Chemosphere* **2010**, *79*, 349–354. [\[CrossRef\]](#)

94. Lusa, M.; Lehto, J.; Aromaa, H.; Knuutinen, J.; Bomberg, M. Uptake of radioiodide by *Paenibacillus* sp., *Pseudomonas* sp., *Burkholderia* sp. and *Rhodococcus* sp. isolated from a boreal nutrient-poor bog. *J. Environ. Sci.* **2016**, *44*, 26–37. [CrossRef]
95. Duborská, E.; Urik, M.; Bujdoš, M. Comparison of iodide and iodate accumulation and volatilization by filamentous fungi during static cultivation. *Water Air Soil Pollut.* **2017**, *228*, 1–8. [CrossRef]
96. Fang, L.; Cai, P.; Chen, W.; Liang, W.; Hong, Z.; Huang, Q. Impact of cell wall structure on the behavior of bacterial cells in the binding of copper and cadmium. *Colloids Surf. A Physicochem. Eng. Asp.* **2009**, *347*, 50–55. [CrossRef]
97. Bhainsa, K.C.; D'Souza, S.F. Thorium biosorption by *Aspergillus fumigatus*, a filamentous fungal biomass. *J. Hazard. Mater.* **2009**, *165*, 670–676. [CrossRef]
98. Fein, J.B.; Daughney, C.J.; Yee, N.; Davis, T.A. A chemical equilibrium model for metal adsorption onto bacterial surfaces. *Geochim. Cosmochim. Acta* **1997**, *61*, 3319–3328. [CrossRef]
99. Gadd, G.M.; White, C. Microbial treatment of metal pollution—A working biotechnology? *Trends Biotechnol.* **1993**, *11*, 353–359. [CrossRef]
100. Mishra, B.; Boyanov, M.; Bunker, B.A.; Kelly, S.D.; Kemner, K.M.; Fein, J.B. High- and low-affinity binding sites for Cd on the bacterial cell walls of *Bacillus subtilis* and *Shewanella oneidensis*. *Geochim. Cosmochim. Acta* **2010**, *74*, 4219–4233. [CrossRef]
101. Antsotegi-Uskola, M.; Markina-Iñarrairaegui, A.; Ugalde, U. Copper resistance in *Aspergillus nidulans* relies on the PI-type ATPase CrpA, regulated by the transcription factor AceA. *Front. Microbiol.* **2017**, *8*, 912. [CrossRef] [PubMed]
102. Orell, A.; Navarro, C.A.; Arancibia, R.; Mobarec, J.C.; Jerez, C.A. Life in blue: Copper resistance mechanisms of bacteria and archaea used in industrial biomining of minerals. *Biotechnol. Adv.* **2010**, *28*, 839–848. [CrossRef]
103. Nies, D.H. Efflux-mediated heavy metal resistance in prokaryotes. *FEMS Microbiol. Rev.* **2003**, *27*, 313–339. [CrossRef]
104. Aro, L.; Korpela, L.; Mäkinen, V.; Salemaa, M.; Saarinen, M.; Lahdenperä, A.M.; Parviainen, L.; Kuusisto, J. *Studies on Reference Mires: 2. Lastensuo, Pesänsuo and Häädetkeidas in 2010–2015; Posiva WR 2017-15; Posiva Oy: Eurajoki, Finland, 2018.*
105. Mäkilä, M.; Grundström, A. *Turpeen ikä ja Kerrostumismopeus Lounais-Suomen Soilla; Working Report 2008–12; Posiva Oy: Eurajoki, Finland, 2008.* (In Finnish)
106. Tsitko, I.; Lusa, M.; Lehto, J.; Parviainen, L.; Ikonen, A.T.; Lahdenperä, A.M.; Bomberg, M. The variation of microbial communities in a depth profile of an acidic, nutrient-poor boreal bog in southwestern Finland. *Open J. Ecol.* **2014**, *4*, 832. [CrossRef]
107. Lusa, M.; Knuutinen, J.; Lindgren, M.; Virkanen, J.; Bomberg, M. Microbial communities in a former pilot-scale uranium mine in Eastern Finland—Association with radium immobilization. *Sci. Total Environ.* **2019**, *686*, 619–640. [CrossRef]
108. Klindworth, A.; Pruesse, E.; Schweer, T.; Peplies, J.; Quast, C.; Horn, M.; Glöckner, F.O. Evaluation of general 16S ribosomal RNA gene PCR primers for classical and next-generation sequencing-based diversity studies. *Nucleic Acids Res.* **2013**, *41*, e1. [CrossRef]
109. Gardes, M.; Bruns, T.D. ITS primers with enhanced specificity for basidiomycetes-application to the identification of mycorrhizae and rusts. *Mol. Ecol.* **1993**, *2*, 113–118. [CrossRef]
110. White, T.J.; Bruns, T.; Lee, S.J.W.T.; Taylor, J. Amplification and direct sequencing of fungal ribosomal RNA genes for phylogenetics. *PCR Protoc. Guide Methods Appl.* **1990**, *18*, 315–322.
111. Edwards, U.; Rogall, T.; Blöcker, H.; Emde, M.; Böttger, E.C. Isolation and direct complete nucleotide determination of entire genes. Characterization of a gene coding for 16S ribosomal RNA. *Nucleic Acids Res.* **1989**, *17*, 7843–7853. [CrossRef] [PubMed]
112. Muyzer, G.; De Waal, E.C.; Uitterlinden, A.G. Profiling of complex microbial populations by denaturing gradient gel electrophoresis analysis of polymerase chain reaction-amplified genes coding for 16S rRNA. *Appl. Environ. Microbiol.* **1993**, *59*, 695–700. [CrossRef] [PubMed]
113. Schloss, P.D.; Westcott, S.L.; Ryabin, T.; Hall, J.R.; Hartmann, M.; Hollister, E.B.; Lesniewski, R.A.; Oakley, B.B.; Parks, D.H.; Robinson, C.J.; et al. Introducing mothur: Open-source, platform-independent, community-supported software for describing and comparing microbial communities. *Appl. Environ. Microbiol.* **2009**, *75*, 7537–7541. [CrossRef]
114. Pruesse, E.; Quast, C.; Knittel, K.; Fuchs, B.M.; Ludwig, W.; Peplies, J.; Glöckner, F.O. SILVA: A comprehensive online resource for quality checked and aligned ribosomal RNA sequence data compatible with ARB. *Nucleic Acids Res.* **2007**, *35*, 7188–7196. [CrossRef] [PubMed]
115. Quast, C.; Pruesse, E.; Yilmaz, P.; Gerken, J.; Schweer, T.; Yarza, P.; Peplies, J.; Glöckner, F.O. The SILVA ribosomal RNA gene database project: Improved data processing and web-based tools. *Nucleic Acids Res.* **2012**, *41*, D590–D596. [CrossRef]
116. Kõljalg, U.; Nilsson, R.H.; Abarenkov, K.; Tedersoo, L.; Taylor, A.F.S.; Bahram, M.; Bates, S.T.; Bruns, T.D.; Bengtsson-Palme, J.; Callaghan, T.M.; et al. Towards a unified paradigm for sequence-based identification of fungi. *Mol. Ecol.* **2013**, *22*, 5271–5277. [CrossRef]
117. Nilsson, R.H.; Larsson, K.-H.; Taylor, A.F.S.; Bengtsson-Palme, J.; Jeppesen, T.S.; Schigel, D.; Kennedy, P.; Picard, K.; Glöckner, F.O.; Tedersoo, L.; et al. The UNITE database for molecular identification of fungi: Handling dark taxa and parallel taxonomic classifications. *Nucleic Acids Res.* **2019**, *47*, D259–D264. [CrossRef]
118. Abarenkov, K.; Zirk, A.; Piirmann, T.; Põhönen, R.; Ivanov, F.; Nilsson, R.H.; Kõljalg, U. UNITE Mothur Release for Fungi. Version 04.02.2020. UNITE Community. 2020. Available online: <https://plutof.ut.ee/#/doi/10.15156/BIO/786381> (accessed on 20 April 2020).
119. Lusa, M.; Bomberg, M.; Aromaa, H.; Knuutinen, J.; Lehto, J. The microbial impact on the sorption behaviour of selenite in an acidic, nutrient-poor boreal bog. *J. Environ. Radioact.* **2015**, *147*, 85–96. [CrossRef] [PubMed]
120. Hammer, Ø.; Harper, D.A.; Ryan, P.D. PAST: Paleontological statistics software package for education and data analysis. *Palaeontol. Electron.* **2001**, *4*, 9.
121. McMurdie, P.J.; Holmes, S. phyloseq: An R package for reproducible interactive analysis and graphics of microbiome census data. *PLoS ONE* **2013**, *8*, e61217. [CrossRef]

122. R Core Team. *R: A Language and Environment for Statistical Computing*; R Foundation for Statistical Computing: Vienna, Austria, 2014; Available online: <http://www.R-project.org/> (accessed on 9 September 2020).
123. Scheller, S.; Goenrich, M.; Boecher, R.; Thauer, R.K.; Jaun, B. The key nickel enzyme of methanogenesis catalyses the anaerobic oxidation of methane. *Nature* **2010**, *465*, 606–608. [[CrossRef](#)] [[PubMed](#)]
124. Madhaiyan, M.; Poonguzhali, S.; Sa, T. Metal tolerating methylotrophic bacteria reduces nickel and cadmium toxicity and promotes plant growth of tomato (*Lycopersicon esculentum* L.). *Chemosphere* **2007**, *69*, 220–228. [[CrossRef](#)] [[PubMed](#)]
125. Ho, Y.S.; Wase, D.J.; Forster, C.F. Batch nickel removal from aqueous solution by sphagnum moss peat. *Water Res.* **1995**, *29*, 1327–1332. [[CrossRef](#)]
126. Vila Domínguez, A.; Ayerbe Algaba, R.; Miró Canturri, A.; Rodríguez Villodres, Á.; Smani, Y. Antibacterial activity of colloidal silver against gram-negative and gram-positive bacteria. *Antibiotics* **2020**, *9*, 36. [[CrossRef](#)]
127. Lusa, M.; Lehto, J.; Bomberg, M. The uptake of Ni²⁺ and Ag⁺ by bacterial strains isolated from a boreal nutrient-poor bog. *AIMS Microbiol.* **2016**, *2*, 120–137. [[CrossRef](#)]
128. Andreasson, A.; Jönsson, B.; Lindman, B. Surface and colloid chemistry of peat and peat dewatering. Electrostatic effects. *Colloid Polym. Sci.* **1988**, *266*, 164–172. [[CrossRef](#)]
129. Strelko, V., Jr.; Malik, D.J. Characterization and metal sorptive properties of oxidized active carbon. *J. Colloid Interface Sci.* **2002**, *250*, 213–220. [[CrossRef](#)] [[PubMed](#)]
130. Corapcioglu, M.O.; Huang, C.P. The adsorption of heavy metals onto hydrous activated carbon. *Water Res.* **1987**, *21*, 1031–1044. [[CrossRef](#)]
131. Tan, K.H. *Humic Matter in Soil and the Environment: Principles and Controversies*, 2nd ed.; CRC Press, Taylor and Francis Group: Boca Raton, FL, USA, 2014; p. 324.
132. Martinez, E.R.; Sharma, P.; Kappler, A. Surface binding site analysis of Ca²⁺-homoionized clay–humic acid complexes. *J. Colloid Interface Sci.* **2010**, *352*, 526–534. [[CrossRef](#)] [[PubMed](#)]
133. Koch-Steindl, H.; Pröhl, G. Considerations on the behaviour of long-lived radionuclides in the soil. *Radiat. Environ. Biophys.* **2001**, *40*, 93–104. [[CrossRef](#)]
134. Huber, R.; Sacher, M.; Vollmann, A.; Huber, H.; Rose, D. Respiration of arsenate and selenate by hyperthermophilic archaea. *Syst. Appl. Microbiol.* **2000**, *23*, 305–314. [[CrossRef](#)]
135. Sarret, G.; Avoscan, L.; Carrière, M.; Collins, R.; Geoffroy, N.; Carrot, F.; Covès, J.; Gouget, B. Chemical forms of selenium in the metal-resistant bacterium *Ralstonia metallidurans* CH34 exposed to selenite and selenate. *Appl. Environ. Microbiol.* **2005**, *71*, 2331–2337. [[CrossRef](#)] [[PubMed](#)]
136. Oremland, R.S.; Hollibaugh, J.T.; Maest, A.S.; Presser, T.S.; Miller, L.G.; Culbertson, C.W. Selenate reduction to elemental selenium by anaerobic bacteria in sediments and culture: Biogeochemical significance of a novel, sulfate-independent respiration. *Appl. Environ. Microbiol.* **1989**, *55*, 2333–2343. [[CrossRef](#)]
137. Handley, K.M.; Verberkmoes, N.C.; I Steefel, C.; Williams, K.H.; Sharon, I.; Miller, C.S.; Frischkorn, K.R.; Chourey, K.; Thomas, B.C.; Shah, M.B.; et al. Biostimulation induces syntrophic interactions that impact C, S and N cycling in a sediment microbial community. *ISME J.* **2013**, *7*, 800–816. [[CrossRef](#)]
138. Nakamaru, Y.M.; Altansuvd, J. Speciation and bioavailability of selenium and antimony in non-flooded and wetland soils: A review. *Chemosphere* **2014**, *111*, 366–371. [[CrossRef](#)]
139. Pettine, M.; Gennari, F.; Campanella, L.; Casentini, B.; Marani, D. The reduction of selenium (IV) by hydrogen sulfide in aqueous solutions. *Geochim. Cosmochim. Acta* **2012**, *83*, 37–47. [[CrossRef](#)]
140. Yeager, C.M.; Amachi, S.; Grandbois, R.; Kaplan, D.I.; Xu, C.; Schwehr, K.A.; Santschi, P.H. Microbial Transformation of Iodine: From Radioisotopes to Iodine Deficiency. *Adv. Appl. Microbiol.* **2017**. [[CrossRef](#)]
141. Fernández-Calviño, D.; Bååth, E. Interaction between pH and Cu toxicity on fungal and bacterial performance in soil. *Soil Biol. Biochem.* **2016**, *96*, 20–29. [[CrossRef](#)]
142. Starr, M.; Lindroos, A.J.; Ukonmaanaho, L.; Tarvainen, T.; Tanskanen, H. Weathering release of heavy metals from soil in comparison to deposition, litterfall and leaching fluxes in a remote, boreal coniferous forest. *Appl. Geochem.* **2003**, *18*, 607–613. [[CrossRef](#)]
143. Moffett, B.F.; Nicholson, F.A.; Uwakwe, N.C.; Chambers, B.J.; Harris, J.A.; Hill, T.C. Zinc contamination decreases the bacterial diversity of agricultural soil. *FEMS Microbiol. Ecol.* **2003**, *43*, 13–19. [[CrossRef](#)]
144. Kour, R.; Jain, D.; Bhojiya, A.A.; Sukhwai, A.; Sanadhya, S.; Saheewala, H.; Jat, G.; Singh, A.; Mohanty, S.R. Zinc biosorption, biochemical and molecular characterization of plant growth-promoting zinc-tolerant bacteria. *3 Biotech* **2019**, *9*, 1–17. [[CrossRef](#)]
145. Myers, B.; Webster, K.L.; Mclaughlin, J.W.; Basiliko, N. Microbial activity across a boreal peatland nutrient gradient: The role of fungi and bacteria. *Wetl. Ecol. Manag.* **2012**, *20*, 77–88. [[CrossRef](#)]
146. Song, N.; Xu, H.; Yan, Z.; Yang, T.; Wang, C.; Jiang, H.L. Improved lignin degradation through distinct microbial community in subsurface sediments of one eutrophic lake. *Renew. Energy* **2019**, *138*, 861–869. [[CrossRef](#)]
147. Lin, X.; Tfaily, M.M.; Steinweg, J.M.; Chanton, P.; Esson, K.; Yang, Z.K.; Chanton, J.P.; Cooper, W.T.; Schadt, C.W.; Kostka, J.E. Microbial community stratification linked to utilization of carbohydrates and phosphorus limitation in a boreal peatland at Marcell Experimental Forest, Minnesota, USA. *Appl. Environ. Microbiol.* **2014**, *80*, 3518–3530. [[CrossRef](#)] [[PubMed](#)]
148. Coolen, M.J.; van de Giessen, J.; Zhu, E.Y.; Wuchter, C. Bioavailability of soil organic matter and microbial community dynamics upon permafrost thaw. *Environ. Microbiol.* **2011**, *13*, 2299–2314. [[CrossRef](#)]